NRC Research and/or Technical Assistance Rept PDR

EGG-CAAD-5860

May 1982

TRAC-BD1 CALCULATION AND DATA COMPARISON OF INTERNATIONAL STANDARD PROBLEM 12

R. J. Dallman

U.S. Department of Energy
Idaho Operations Office • Idaho National Engineering Laboratory

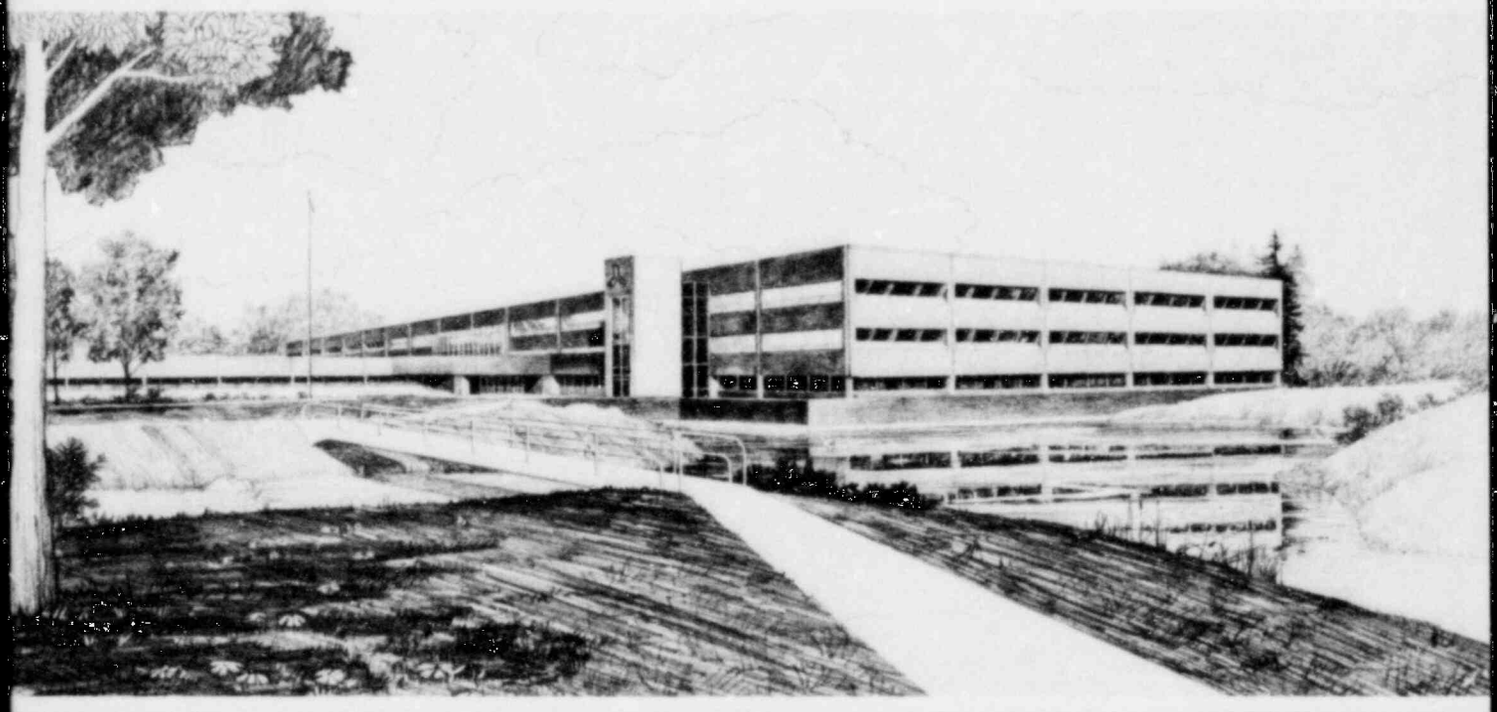

Prepared for the U.S. Nuclear
Regulatory Commission under
DOE Contract No. DE-AC07-76ID01570
NRC FIN No. A6047

EG&G Idaho

EG&G Idaho, Inc.

FORM EG&G 398
(Rev. 03-82)

INTERIM REPORT

Accession No. _____

Report No. EGG-CAAD-5860

Contract Program or Project Title: NRC Technical Assistance Program Division

Subject of this Document: TRAC-BD1 CALCULATION AND DATA COMPARISON OF INTERNATIONAL STANDARD PROBLEM 12

Type of Document: Technical Report

Author(s): R. J. Dallman

Date of Document: May, 1982

Responsible NRC Individual and NRC Office or Division: F. Odar, NRC-RSR

EG&G Idaho, Inc.
Idaho Falls, Idaho 83415

Prepared for the
U.S. Nuclear Regulatory Commission
Washington, D.C.
Under DOE Contract No. DE-AC07-76ID01570
NRC FIN No. A6047

INTERIM REPORT

ABSTRACT

A best-estimate, TRAC-BD1 computer simulation and subsequent code/data comparison was conducted for Run 912 of the ROSA-III small break LOCA test series. This work was primarily performed for the United States Nuclear Regulatory Commission's participation in International Standard Problem 12. This work also serves a secondary role through its applicability to the Nuclear Regulatcry Commission's code assessment objectives. Results from the code-calculated behavior, with comparisons to the experimental data, are presented. Conclusions relative to the code usage and performance, and recommendations for potential code improvement are given.

Code Assessment and Applications

NRC FIN No. A6047

SUMMARY

A TRAC-BD1 code calculation of Run 912 from the ROSA-III small break LOCA test series was performed at the INEL for the United States Nuclear Regulatory Commission. The primary objective of this work was to provide calculational results for inclusion in International Standard Problem 12. A secondary objective was to assess the capabilities of TRAC-BD1 to predict an integral simulation of a small break LOCA.

Several sensitivity calculations were made which yielded information relative to the use of certain code options and modeling techniques. Code updates were incorporated which improved the reliability of TRAC-BD1, and enabled the calculation to be successfully completed.

Major conclusions resulting from the calculation are summarized as follows:

1. Overall data trends and system behavior were predicted well by TRAC-BD1.

2. Calculated event timing based on downcomer level and system pressure compared favorably with the data.

3. Predicted rod surface temperatures indicated two anomalous heatups. They were caused by overpredictions of bundle void fractions during portions of the transient.

4. The proper modeling of ambient heat loss during a small break test in ROSA-III is very important. TRAC-BD1 capabilities in this area should be expanded.

5. During dryout conditions, TRAC-BD1 predicted rod heatup rates which were lower than those in the data. The cause of this difference should be investigated.

6. When setting up a TRAC-BD1 model, care should be taken to accurately model vessel pipe connections which have the potential for fluid flashing.

ACKNOWLEDGEMENT

The author expresses appreciation to Dawnie Judd for her assistance in generating plots and nodalization drawings.

CONTENTS

FIGURES

TABLES

TRAC-BD1 CALCULATION AND DATA COMPARISON OF INTERNATIONAL STANDARD PROBLEM 12

1. INTRODUCTION

International Standard Problem (ISP) 12 consists of a single small break Loss-of-Coolant Accident (LOCA) test performed in the Rig of Safety Assessment (ROSA)-III experimental facility. ROSA-III is one of several Boiling Water Reactor (BWR) research programs conducted by the Japan Atomic Energy Research Institute (JAERI). The test chosen for ISP 12 was Run 912 which simulated a 5% split break at the recirculation pump inlet with an assumption of a High Pressure Core Spray (HPCS) diesel generator single failure.

This document describes the TRAC-BD1 computer code simulation of the selected data. Because ISP 12 is an open standard problem (i.e. the experimental data was available prior to the code simulation) the code calculated performance of significant system parameters is also compared with the test data. Section 2 of this document gives descriptions of the test facility and specific test to that detail necessary for an understanding of the computer model (Section 3), boundary conditions (Section 3), and calculated results (Section 4). The code/data comparisons are also included in Section 4. Conclusions relative to code usage, performance, and potential improvements are given in Section 5. References are listed in Section 6.

2. FACILITY AND TEST DESCRIPTION

2.1 Facility Description

The ROSA-III facility is a volumetrically scaled (1/424) simulated BWR system with an electrically heated core. The design goal of the facility is to produce the significant thermal-hydraulic phenomena in the same sequence, general time frames, and appropriate magnitudes as would occur in a BWR. The major components and subsystems contained in ROSA-III are shown pictorially and schematically in Figures 1 and 2, respectively.

As Figure 2 illustrates, two symmetrical recirculation loops are provided. Each loop contains a recirculation pump and two jet pumps. The simulated broken loop is equipped with a sharp-edged orifice and a quick opening blowdown valve.

A typical BWR emergency core cooling system (ECCS) is simulated, with HPCS and low pressure core spray (LPCS) injected into the upper plenum. Low pressure coolant injection (LPCI) injects through a circular sparger in the upper core bypass region. The automatic depressurization system (ADS) is simulated in one branch of the steam line. Also located in the steam line are a simulated main steam isolation valve (MSIV) and a safety relief valve (SRV).

The pressure vessel internals are illustrated in Figure 3. Pertinent elevations are shown in mm from the vessel bottom. In Figure 4 are shown the steady state coolant flow paths in the vessel and ECC flows during a LOCA.

Four half-length electrically heated bundles make up the ROSA-III simulated core. Each bundle contains 62 heated rods and 2 water rods in an 8 x 8 array. One bundle represents a high power bundle and the others average power bundles. The radial power distribution is shown in Figure 5, and the chopped cosine axial power distribution in Figure 6.

2.2 Test Description

Run 912 simulated a 5% break of one recirculation suction line, and assumed the failure of the HPCS. Measured initial and test conditions for Run 912 are summarized in Table 1, and Table 2 lists the sequence of events.

Following the break initiation which started the transient, a long subcooled blowdown was observed. System pressure was dominated by flow through the steam line, first decreasing then rapidly increasing when the MSIV closed. SRV operation kept the pressure below 8.47 MPa. The ADS valve opened at 158 s, which resulted in a rapid system depressurization. Rod heatup began around 200 s as the bundles dried out. LPCS was initiated at 318 s and LPCI at 406 s. All heater rods were quenched by 444 s and the core was reflooded. Key data parameters are presented in Section 4 and compared to calculated results.

3. TRAC-BD1 MODEL DESCRIPTION

In this section, descriptions are provided for the code version, the model nodalization, and the code options. Also, the formulations of boundary conditions used in the calculation are described.

3.1 Computer Code Description

TRAC-BD1 (Reference 2) is an advanced best estimate computer program for BWR LOCA analysis. Version 11[a] of the code was originally chosen for the ISP 12 calculation. However, reliability problems with that version forced an early termination of the calculation. Error corrections and some model improvements were subsequently added to Version 11 in the form of code updates.[b] These updates enabled the calculation to be successfully completed, and they were incorporated into Version 12 of TRAC-BD1. The TRAC-BD1 input deck is stored at the INEL under Configuration Control Number F00841.

3.2 Nodalization

The TRAC-BD1 vessel nodalization of ROSA-III is illustrated in Figure 7. Twelve axial levels and three radial rings were provided in this two-dimensional vessel (no azimuthal dependency). The core and bypass regions were modeled by the two inner rings in Levels 4 through 7. A CHAN component in the inner ring was used to simulate the high power bundle in ROSA-III (channel box "A"). In the second ring, one CHAN simulated the three average power bundles (channel boxes, "B", "C", and "D").

Each CHAN contained ten cells in the axial direction. The bottom cell represented the volume between the side entry orifice (SEO) and the bottom of the heated length (BHL). This cell was 0.428 m in length and contained

---

a. Filed under INEL Computer Code Configuration Control No. F00814.

b. Filed under INEL Computer Code Configuration Control No. F00842.

the leakage path between the bundle and bypass regions. The next eight cells represented the heated length of the channels. They were all 0.235 m in length to correspond to the axial power distribution of the heater rods (see Figure 8). The upper cell represented part of the unheated channel box extensions.

Radial power distribution was accounted for in the "hot" CHAN by specifying four rod groups. Three groups corresponded to the different peaking factors shown in Figure 5, and the fourth modeled two water rods. In the "average" CHAN, one rod group modeled all of the heated rods with a radial peaking factor of 1.0.

The remaining vessel regions including the guide tube, lower and upper plenums, steam separator, steam dome, and downcomer were also simulated. Cell volumes and axial flow areas in the middle and inner rings were scaled on a ratio of 3 to 1. This corresponded to the number of bundles simulated in each of the two rings. Radial flow areas were unrestricted between the two inner rings. Radial flow areas between the middle and outer rings were zero except in levels 1, 10, and 12. In level 10 (steam separator), only liquid could flow between the middle and outer rings. In levels 1 and 12, vapor and liquid flows were unrestricted.

The TRAC-BD1 system nodalization of ROSA-III is illustrated in Figure 9. Both the intact and broken recirculation loops were modeled. One JET PUMP component in each loop simulated two experimental jet pumps. Zero-velocity FILL components (components 80 and 81) provided proper boundary conditions (no flow) for the guide tube bottoms. The components simulating the feedwater, ECC, and steam line boundary conditions are described in Section 3.4.

3.3 Code Options

Main program control options include convergence criteria and maximum numbers for numerical iterations. These numbers were all input per their recommended values (Reference 2). Two other options in the main control are the conduction boundary condition (fully-implicit option used) and the water packing option (not used).

The critical flow model was used at the jet pump drive nozzles throughout the transient, and at the break plane after 111 s. Before 111 s, the calculated break flow was subcooled. Because of oscillations experienced during subcooled blowdown, the critical flow model was not used. Instead, break flow was derived during that period from the momentum equation solution.

The countercurrent flow limiting (CCFL) model with SEO coefficients was utilized at the inlet of both CHAN components. The CCFL model with upper tie plate (UTP) coefficients was used at junctions which represented upper and lower tie plates, guide tube/bypass interfaces, and bypass/upper plenum interfaces.

In the CHAN components, several user-specified heat transfer options are provided. Critical heat flux (CHF) was calculated with the maximum of the Biasi and Biasi critical quality CHF correlations. The minimum stable film boiling point was taken to be the maximum of those calculated by the homogeneous nucleation and Iloeje correlations. A threshold void fraction value of 0.9 was used for the radiation calculation. The calculation included steam and droplets, and correct view factors were used for anisotropic reflection.

3.4 Boundary Conditions

As shown in Figure 2, the ROSA-III facility has one steam line penetration which branches into three parallel lines. These lines simulate the operation of the MSIV, SRV, and ADS. To simplify the TRAC-BD1 model, three vessel connections were provided (see Figure 9) for these systems. Each connection consisted of a PIPE and a FILL component, and they are described below.

Components 52 and 53 modeled the steam line flow for the first 23 s. Flow was input from the data (Reference 3) as a velocity versus time boundary condition. At 23 s the MSIV was completely closed. Components 58 and 59 modeled flow through the SRV. The input was a velocity versus pressure boundary condition which allowed steam flow when the system pressure exceeded 8.40 MPa, and insured the pressure remained below

8.47 MPa. The ADS flow was modeled with components 60 and 61, and was activated with a downcomer level trip (4.25 m from the vessel bottom). After a 120 s delay, the flow was input as a velocity versus pressure boundary condition to match the data.

LPCS and LPCI flows were both input as velocity versus pressure boundary conditions. LPCS was activated when the system pressure reached 2.38 MPa, and LPCI at 1.81 MPa. The flows were each proportioned, with 1/4 of the total flow entering the inner vessel ring and 3/4 into the middle ring.

3.5 Calculational Sensitivities

While initializing the TRAC-BD1 input deck and during several partial calculations, modeling and nodalization sensitivities were observed. These are described in the following four subsections.

3.5.1 Jet Pumps

As noted in Section 3.2, one JET PUMP component was utilized in both recirculation loops, and each modeled two jet pumps. During the initialization process, it was observed that the calculated M-ratios were underpredicted. While the number of cells in a JET PUMP component is fixed, the code user has some freedom to adjust various loss coefficients. By adjusting these loss coefficients along with loop differential pressures, a calculated M-ratio of 1.5 was obtained. The initial measured M-ratio was 1.8. Therefore, the initial recirculation pump speeds had to be input at higher values than the data in order to obtain the correct initial core inlet flow. The pump speeds during coastdown were input from the data, normalized to their higher initial values.

In TRAC-BD1, the JET PUMP component was developed partially from 1/6-scale and prototypical jet pump data. These data were taken from jet pumps which were located within pressure vessels. As such, certain assumptions were made concerning the orientation and momentum of the suction flow. These assumptions may not be totally applicable for different geometries, such as the external jet pumps found in ROSA-III. It

is also possible that by allowing variations in cell nodalization, the JET PUMP component would provide added flexibility to match data from different jet pump configurations.

3.5.2 Break Flow

It was concluded in Reference 4 that calculated break flows were dependent on how the break was nodalized. Following the recommendations in that reference, the cell upstream of the break plane was modeled as a truncated core (Figure 10). The break plane represented the proper flow area associated with the break orifice (0.0059-m dia.). During the subcooled portion of the blowdown, the critical flow model caused flow oscillations and was not used. However, when the calculated upstream conditions became saturated (111 s) the critical flow model was applied at the break plane.

Note in Figure 10 that the hydraulic diameter at the break plane was identical to that used at the upstream junction. Using the value of the hydraulic diameter which represented the orifice flow area resulted in a very high wall shear, and consequently an underpredicted subcooled break flow rate. Using the upstream value at the break plane produced good results.

3.5.3 Ambient Heat Loss

Heat loss tests have indicated that the ROSA-III facility loses approximately 150 kW to the ambient when it is at steady state pressure and temperature. This heat loss decreases linearly as a function of the temperature difference between the system fluid (at steady state) and the ambient. The distribution of this heat loss from the facility has not been quantified.

Since the ambient heat loss would represent a large percentage of the decay power during portions of the transient, its modeling was deemed important. Originally the entire heat loss was calculated to occur through the vessel. This was accomplished by using a double-sided heat slab to represent the vessel wall at each axial elevation. The ambient temperature

was set at 294 K, and the vessel outside surface heat transfer coefficient varied until the initial heat loss was obtained. This resulted in high condensation rates in the vessel as steam contacted "cool" vessel inner walls. The system pressure remained much lower than the data, and the downcomer liquid inventory was partially sustained.

There are two primary reasons why high condensation rates were calculated. First, TRAC-BD1 allows only one material for a double-sided slab. Thus, the proper thermal resistance (metal plus insulation) through the vessel cannot be properly modeled. Second, the ambient temperature and outer surface heat transfer coefficient are constant for each elevation. This forces the heat loss to be dependent on surface area, and precludes, for instance, the modeling of dense vessel penetrations.

It was felt that some distribution of the heat loss between the vessel and recirculation loops was required. After examining surface areas and instrument penetrations, the heat loss was modified to give initial values of 95 kW from the loops and 49 kW from the vessel. The fact that the recirculation pumps in ROSA-III are not insulated also influenced the final distribution. The effects of this heat loss on the final calculation are discussed in Section 4.

3.5.4 Feedwater

A review of the data indicated that the system pressure was held up around the time that LPCS came on. Closer examination revealed that the pressure hold up could be partially caused by flashing of the fluid in the feedwater line. A sensitivity calculation confirmed this, and the feedwater line was properly modeled from the vessel to the isolation valve. Feedwater flow for the first 4 s was input as a velocity versus time boundary condition to match the data.

4. CALCULATIONAL RESULTS

In this section, pertinent TRAC-BD1 calculated parameters are presented and discussed. Where applicable, comparisons of calculated results are made with data (Reference 3). These data were received prior to a detailed analysis and interpretation by the experimenter. As such, the data presented here should be considered as preliminary. Where measurement uncertainties were known, they are included on the figures.

Calculated steam dome pressure is shown in Figure 11 compared with data. The pressure remained fairly constant until the power decay (see Figure 12) began at 8.8 s. It then decreased rapidly until MSIV closure at 23 s. Following steam line closure, the pressure increased and was held below 8.47 MPa by the SRV. The ADS was calculated to open at 164 s (158 s in experiment), which resulted in a rapid steam blowdown. Calculated pressure subsequently matched the data well until LPCS came on at 327 s (318 s in experiment). In the experiment, steam generation caused by LPCS encountering hot heater rods held up the pressure and delayed LPCI initiation until 406 s. In the calculation, the heater rods were not as hot, and less steam was generated by the LPCS. As a result, the pressures diverged and calculated LPCI initiation was at 367 s. The calculated pressure spike at 400 s was caused by the simultaneous quenching of heater rods, which released a large amount of energy to the bundle fluid.

Steam line flows are shown in Figure 13. Calculated SRV flow is shown between 47 and 86 s. Experimental SRV flow was not available for plotting, however, it was approximately 0.2 kg/s from 84 to 109 s. A 6 s offset is observed between calculated and actual ADS initiation. This corresponded to the difference between calculated and actual Level 1 signals.

Flows through the break orifice are compared in Figure 14. The calculated break flow went from subcooled to saturated at 111 s, which caused the dramatic decrease in mass flow. The data indicated a subcooled break flow until ADS initiation at 158 s. Because of the high data uncertainties, it is not clear whether the calculated break flow was over-

or underpredicted. The early calculated transition to saturated flow, however, would be indicative of an overprediction.

An important factor in predicting the break flow transition is ambient heat loss from the vessel. Early sensitivity calculations revealed that the ADS downcomer level trip was delayed by 23 s, when all of the ambient heat loss was taken from the vessel versus no heat loss from the vessel. This dramatic difference is attributed to the following. For the case of total heat loss from the vessel, significant steam condensation occurred in the steam dome and downcomer. This provided an effective source of liquid to the downcomer, and delayed the level trip. It would also delay the time at which steam would reach the break.

As explained in Section 3.5.3, the TRAC-BD1 model was initialized by removing 1/3 of the ambient heat loss from the vessel. From the above discussion it appears that ratio was low. Also, by removing more energy from the vessel, the calculated repressurization (Figure 11) after MSIV closure would have been less severe and compared better with the data. Following the same argument, break flow transition would have been delayed, resulting in a better pressure prediction prior to ADS initiation.

The initiation and subsequent magnitude of the ECC flows (LPCS and LPCI) are functions of the system pressure. As shown in Figure 15, calculated LPCS initiation occurred at 327 s (318 s in the data). Calculated LPCI initiation was at 367 s compared to 406 s in the data.

Figure 16 illustrates total core inlet mass flow rates for the first 100 s. The data is only valid for single phase liquid flow, and is not shown after 100 s. Between 5 and 20 s, the calculated flow underpredicted the data. This was caused primarily because TRAC-BD1 underpredicted the jet pumps M-ratios. In the calculation, the recirculation pump speeds were input as speed versus time to match the data. Thus, the drive flow was correct, but the jet pump suction flow was too low. This resulted in the jet pump discharge flow, and consequently the core inlet flow, to be underpredicted during the pump coastdown period (0-10 s).

Because TRAC-BD1 does not calculate liquid levels, they must be deduced from regional void fractions. In Run 912, void fractions were not measured. Instead, liquid levels in the pressure vessel were estimated from conductivity probes. These liquid levels are shown in Figure 17, and provide indirect comparsions to calculated regional void fractions. Bypass instrumentation was not present in ROSA-III, therefore, no levels are given for that region.

In Figure 18, a comparison is shown of calculated and experimental downcomer heads. The calculation shows the downcomer emptied to the recirculation suction line at 111 s, whereas in the data this occurred at 155 s. As discussed previously this difference was due to the effects of break flow and ambient heat loss. The calculation indicates an earlier refill of the downcomer, and is directly attributable to the earlier predicted LPCI initiation.

Calculated void fractions in the lower plenum are shown in Figure 19. ADS initiation at 164 s caused flashing, which is illustrated by the rapid increase in void fraction throughout the lower plenum. The upper level of the lower plenum (Level 3 in Figures 7 and 19) was totally voided by 225 s. The void fractions steadily increased until LPCI initiation, subsequently the lower plenum was totally refilled by 470 s. Comparing these results to Figure 17, it is seen that TRAC-BD1 predicted higher voids than those shown in the data. The lower plenum liquid level dropped to the recirculation suction line elevation at 325 s. This is equivalent to Level 3 in the calculation voiding out, which occurred at 225 s.

Calculated void fractions in the upper plenum are shown in Figure 20. Level 8 (see Figure 7) is shown to contain a considerable amount of liquid until 200 s. Conversely, Figure 17 indicates that the upper plenum was totally drained by 125 s. This leads to the conclusion that TRAC-BD1 underpredicted liquid drainage from the upper plenum into both the bypass and channels. This is further supported by Figures 21 and 22, which show vapor and liquid velocities at the UTP in the "hot" and "average" CHANs, respectively. No liquid was calculated to penetrate from the upper plenum

into the channels until after 400 s. This result is independent of the CCFL model, and was caused simply by a slip velocity which would not allow liquid downflow.

Rod thermocouple (TC) data are compared to a calculated rod surface temperature in Figure 23. Curves shown correspond to TC position 3 and TRAC-BD1 CHAN cell 7 (see Figure 8). The experimental data consist of the mean of all high powered rods in Channel "A", and in addition, the minimum and maximum of those data. The calculated curve corresponds to the high powered rod group in the hot CHAN. Several obvious differences between the data and calculation are observed. A calculated heatup beginning at 7 s was not seen in the data. This is attributed to the underpredicted core inlet flow (Figure 16) discussed earlier. The second calculated heatup which began at 80 s was not observed in the data. This heatup was caused by the channel drying out, and would probably have been prevented if upper plenum liquid had drained into the channel. This heatup was terminated as liquid flowed into the channels following ADS initiation (and lower plenum flashing). As shown in Figure 17, the actual bundles began to uncover at 200 s, followed shortly by rod heatups. In the calculation, continued flashing through the channels and liquid hold up there delayed the final rod heatup. In the experiment, some rods were quenched from top down spray, and the remainder from bottom reflood. In the calculation, bottom reflood caused the rod quench.

The effect of calculated fluid conditions on rod surface temperatures is illustrated by Figure 24. Following the previous discussions, the rods heated up when the bundle voided, but stayed near saturation temperature when liquid was held up in the bundle.

All rod groups in the hot CHAN showed similar behavior (Figure 25), with the exception of the first calculated heatup. The average-powered rods showed a reduced heatup, and the low-powered rods did not show it at all. A comparison of the rods in the average CHAN to the high-powered rods in the hot CHAN (Figure 26) indicates similar behavior. The rods in the average CHAN did not experience an early heatup.

In the experiment, the rod TCs indicated similar trends at all axial elevations. Heatups occurred between 200 and 275 s as the bundles voided. Quenches were observed between 325 and 440 s. In the calculation, the rods in the lower three CHAN cells (Figure 8) did not heatup. This was caused by high interfacial shear values which limited the liquid draining to the lower plenum.

Differences between measured and calculated rod temperatures have been explained by improperly calculating fluid conditions in the bundles. High interfacial shear values in TRAC-BD1 prevented liquid from draining into the bundles from the upper plenum during the early part of transient. Later in the calculation, the bundles were prevented from completely draining into the lower plenum. Figure 27 illustrates a temperature difference not attributable to fluid conditions. In the figure are shown the mean, mimimum, and maximum hot rod data compared to the calculated value at TC position 2 (see Figure 8). Between 250 and 370 s, the CHAN cell corresponding to the plotted rod temperature was totally void of liquid. The calculated heatup rate, however, was much less than in the data. The specific reason for this is not known, but it involves the TRAC-BD1 heat transfer package and should be investigated.

5. CONCLUSIONS

Overall data trends and system behavior were predicted well by TRAC-BD1.

Calculated event timing based on downcomer level and system pressure compared favorably with the data.

Predicted rod surface temperatures indicated two anomalous heatups. They were caused by overpredictions of bundle void fractions during portions of the transient.

The JET PUMP component in TRAC-BD1 may need added flexibility to properly model unusual geometries such as those found in ROSA-III. The calculated M-ratios could not be made to match the data with existing user input.

The proper modeling of ambient heat loss with TRAC-BD1 is important. System behavior is very sensitive to heat loss distribution. TRAC-BD1 capabilities in this area should be expanded.

When setting up a TRAC-BD1 model, care should be taken to accurately model vessel pipe connections which have the potential for fluid flashing.

During dryout conditions, TRAC-BD1 predicted rod heatup rates which underpredicted the data. The cause of this difference should be investigated.

6. REFERENCES

1. Yoshinari Anoda et al., ROSA-III System Description for Fuel Assembly No. 4, JAERI-M 9363, February 1981.

2. J. W. Spore et al., TRAC-BD1: An Advanced Best Estimate Computer Program for Boiling Water Reactor Loss-of-Coolant Accident Analysis, NUREG/CR-2178, EGG-2109, October 1981.

3. Yoshinari Anoda et al., Experiment Data of ROSA-III Integral Test Run 912 (5% Split Break Test Without HPCS Actuation), JAERI Data Report, July 1981.

4. R. G. Hanson, TRAC-BD1 Assessment Calculations for Marviken Tests 15 and 24, EGG-CAAD-5705, December 1981.

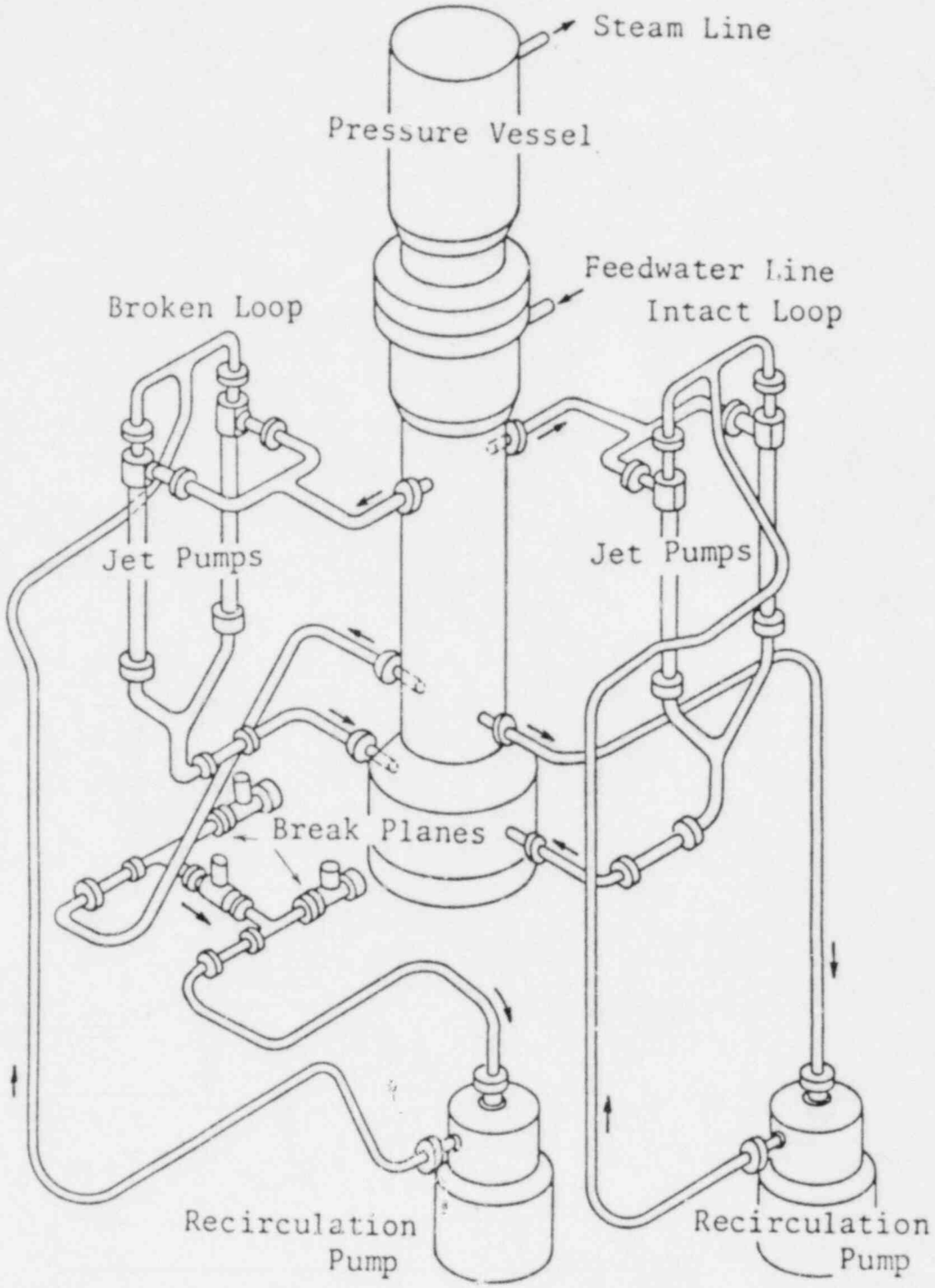

Figure 1. Pictorial diagram of the ROSA-III test facility.[1]

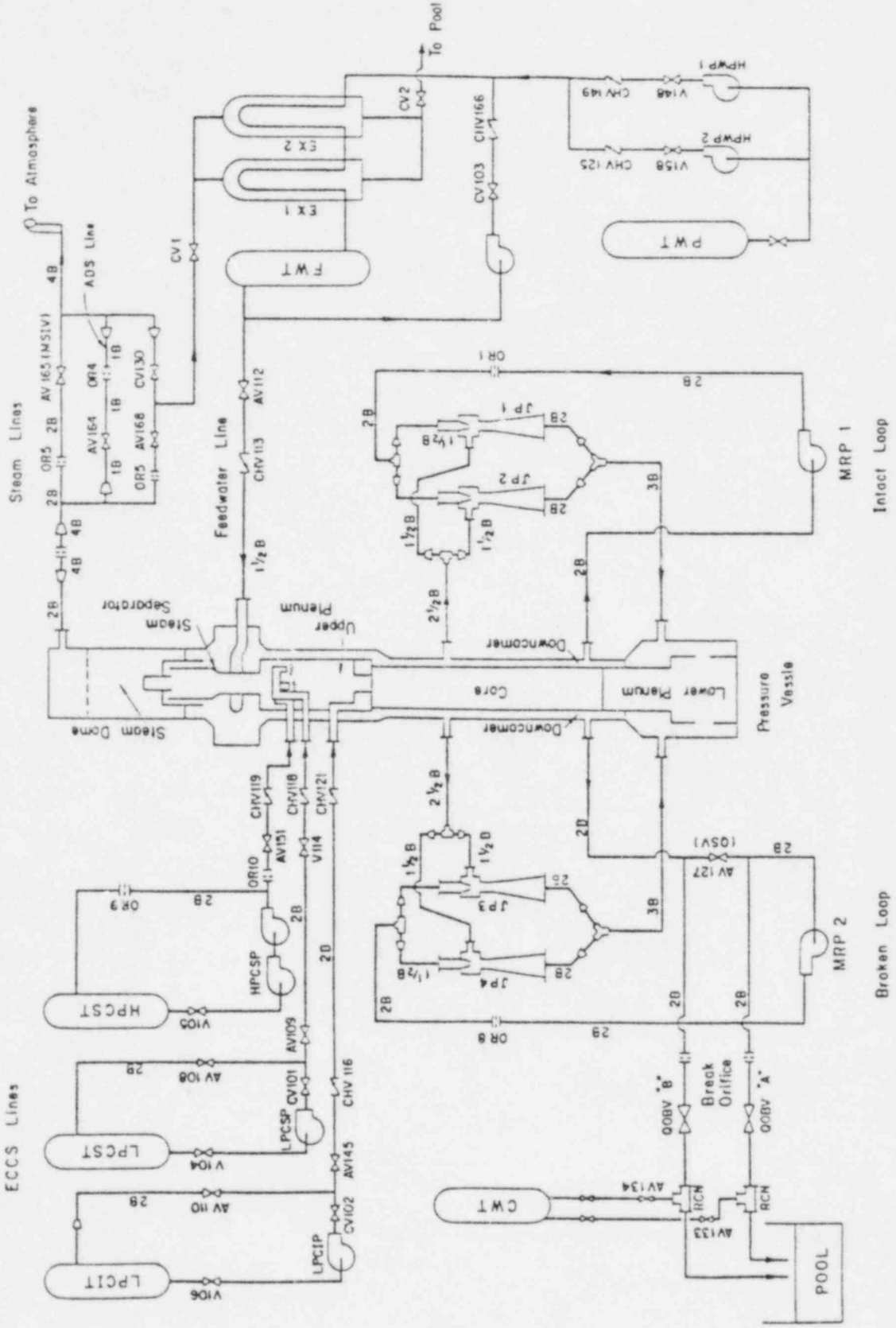

Figure 2. ROSA-III schematic.[1]

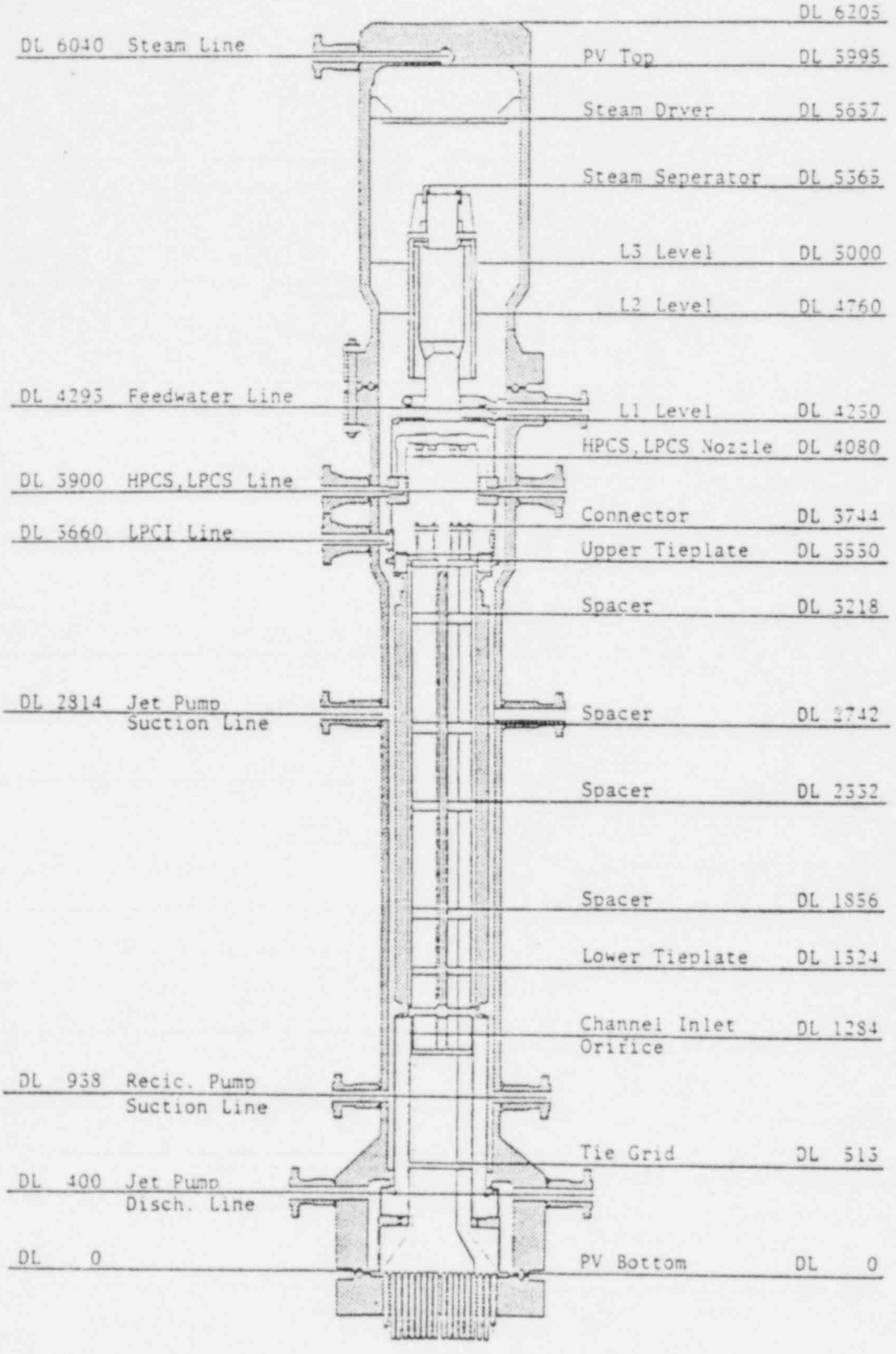

Figure 3. Pressure vessel internals.[1]

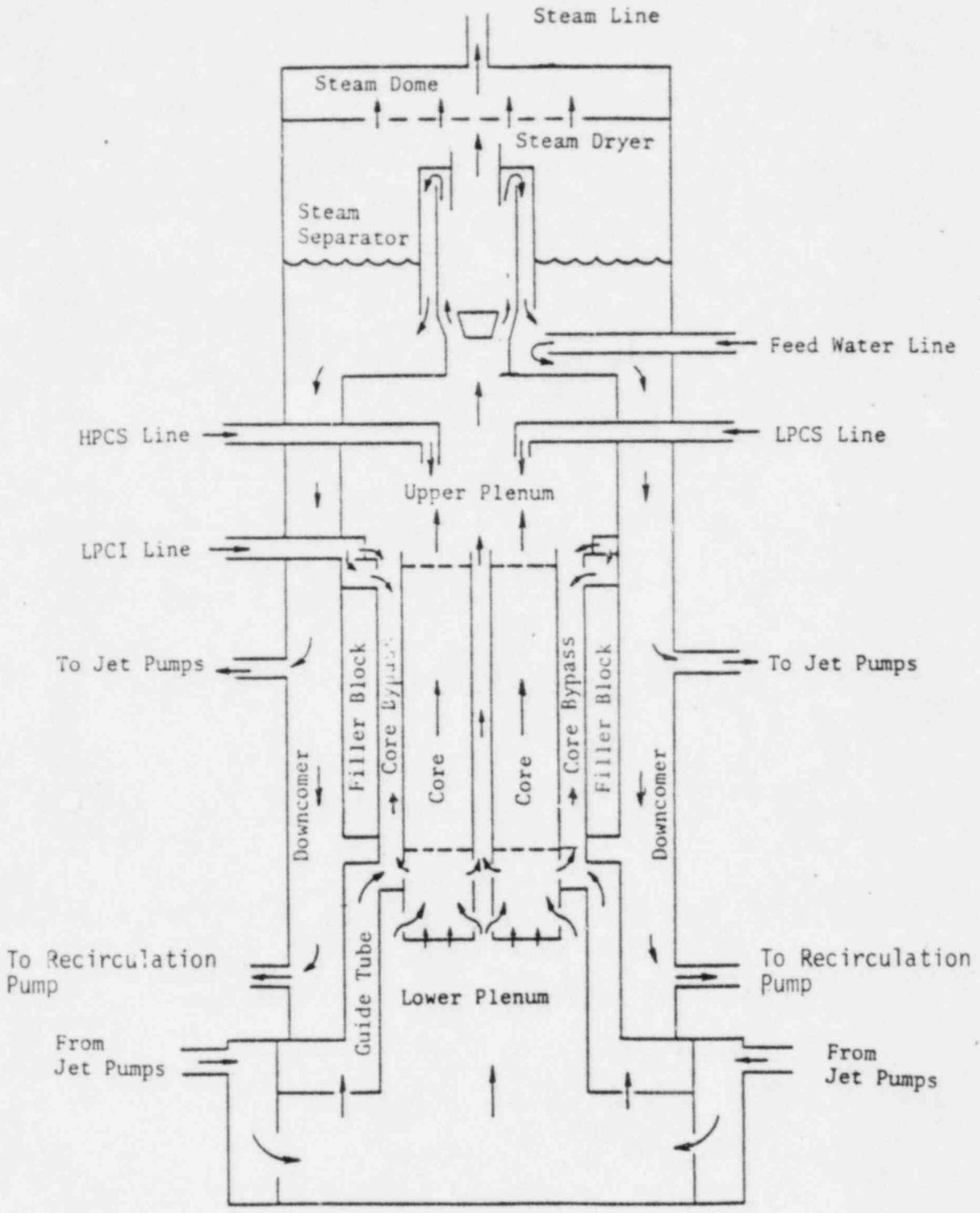

Figure 4. Steady state coolant flow in the vessel and ECC flow during LOCA.[1]

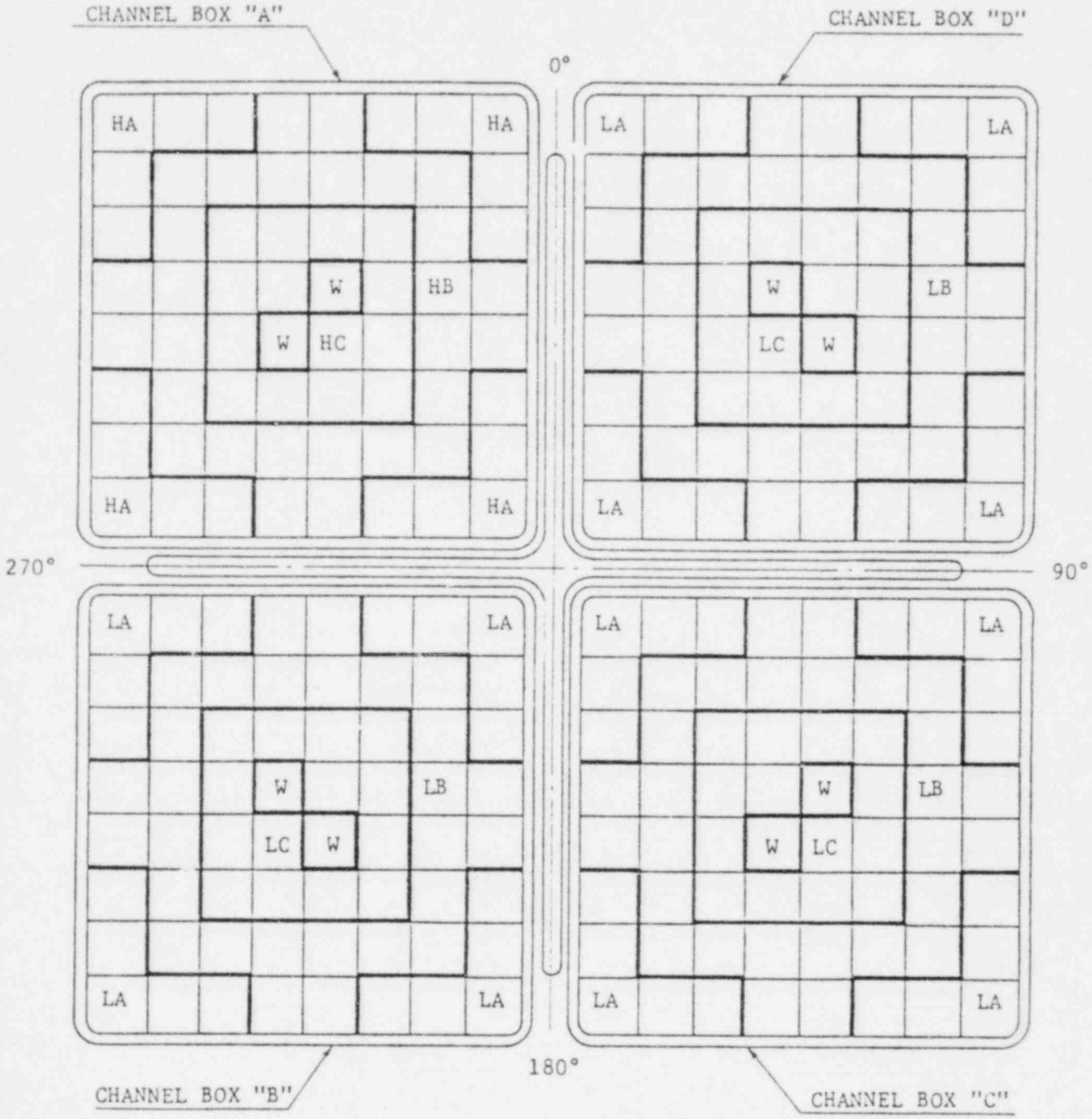

Region	HA	HB	HC	LA	LB	LC	W
Lenear Heat Rate (kW/m)	18.5	16.81	14.41	13.21	12.01	10.29	0.0
Local peaking factor	1.1	1.0	0.875	1.1	1.0	0.875	0.0
No. of Rods	20	28	14	60	84	42	8

* note : Radial peaking factor is 1.4

Figure 5. ROSA-III radial power distribution.[1]

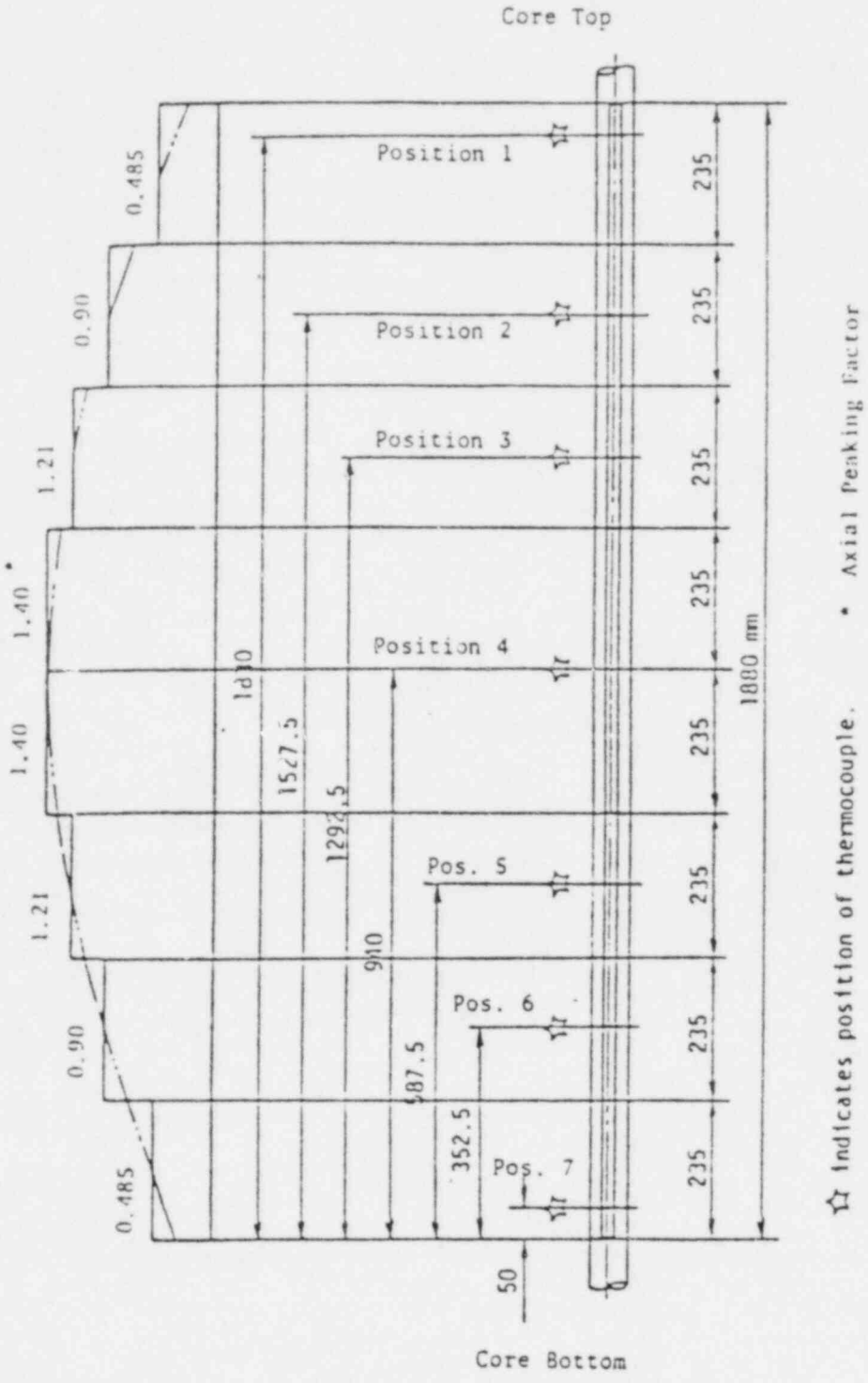

Figure 6. ROSA-III axial power distribution.[1]

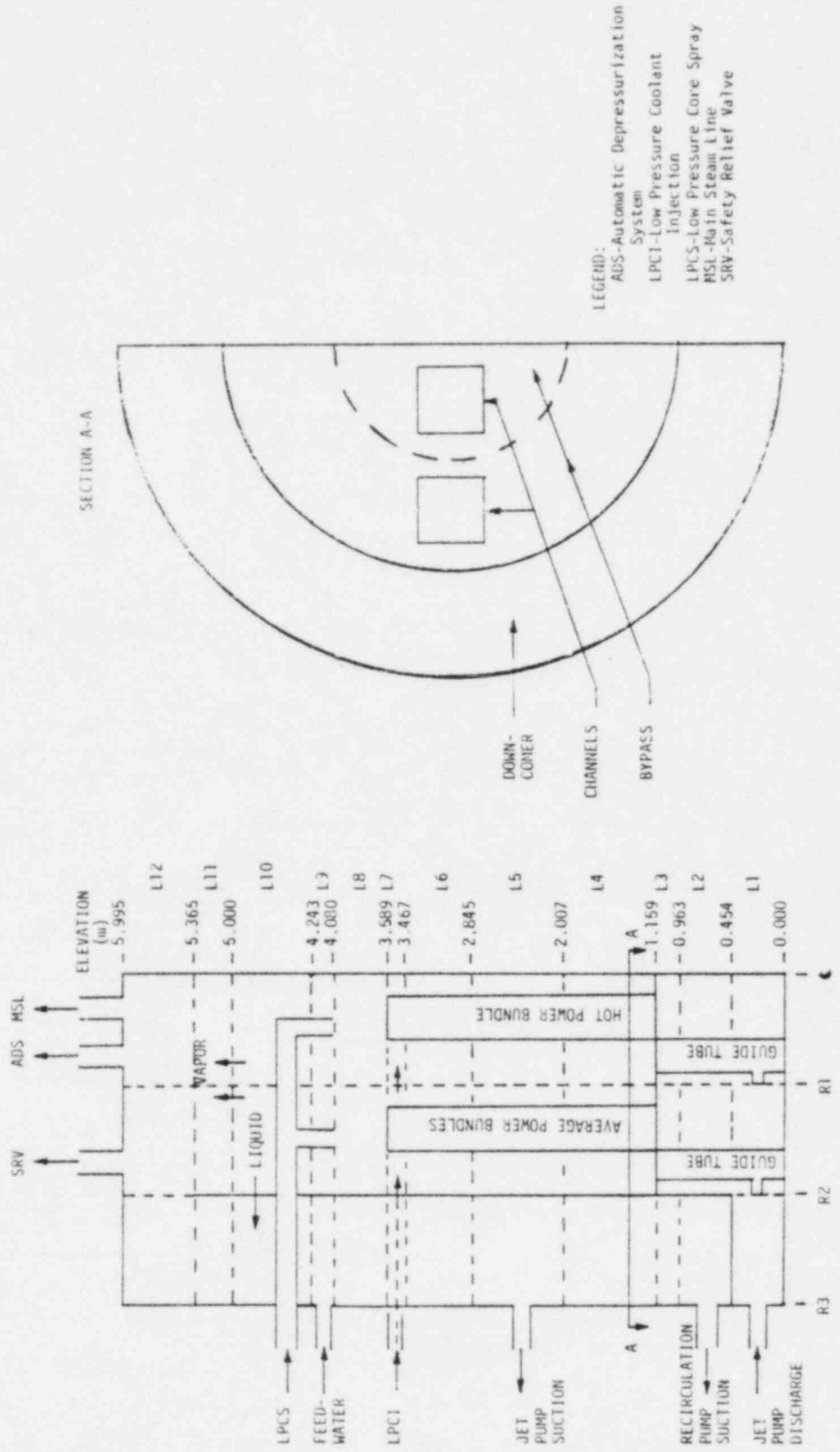

Figure 7. TRAC-BD1 vessel nodalization of ROSA-III.

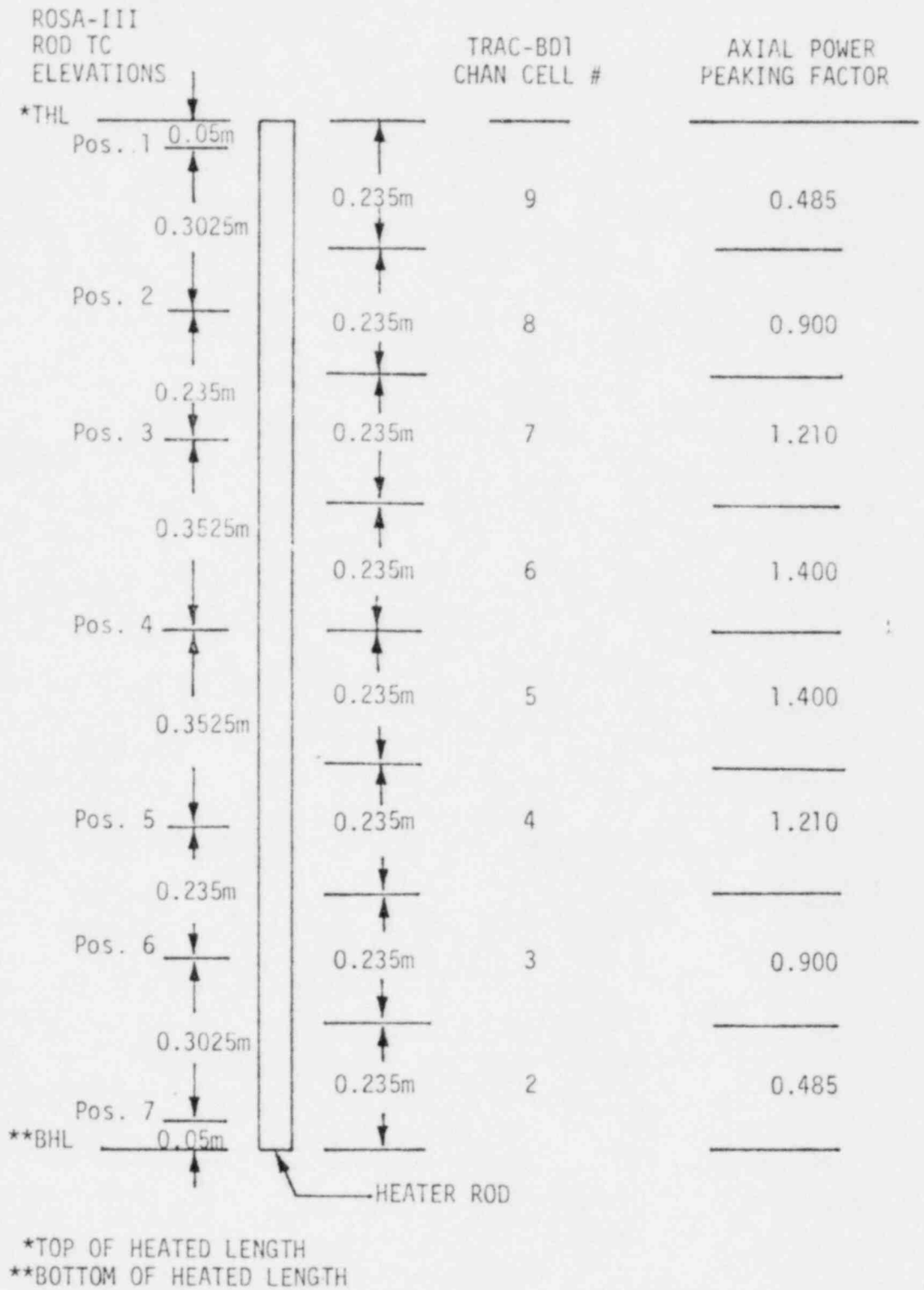

Figure 8. TRAC-BD1 CHAN heated cell elevations compared to ROSA-III thermocouple locations.

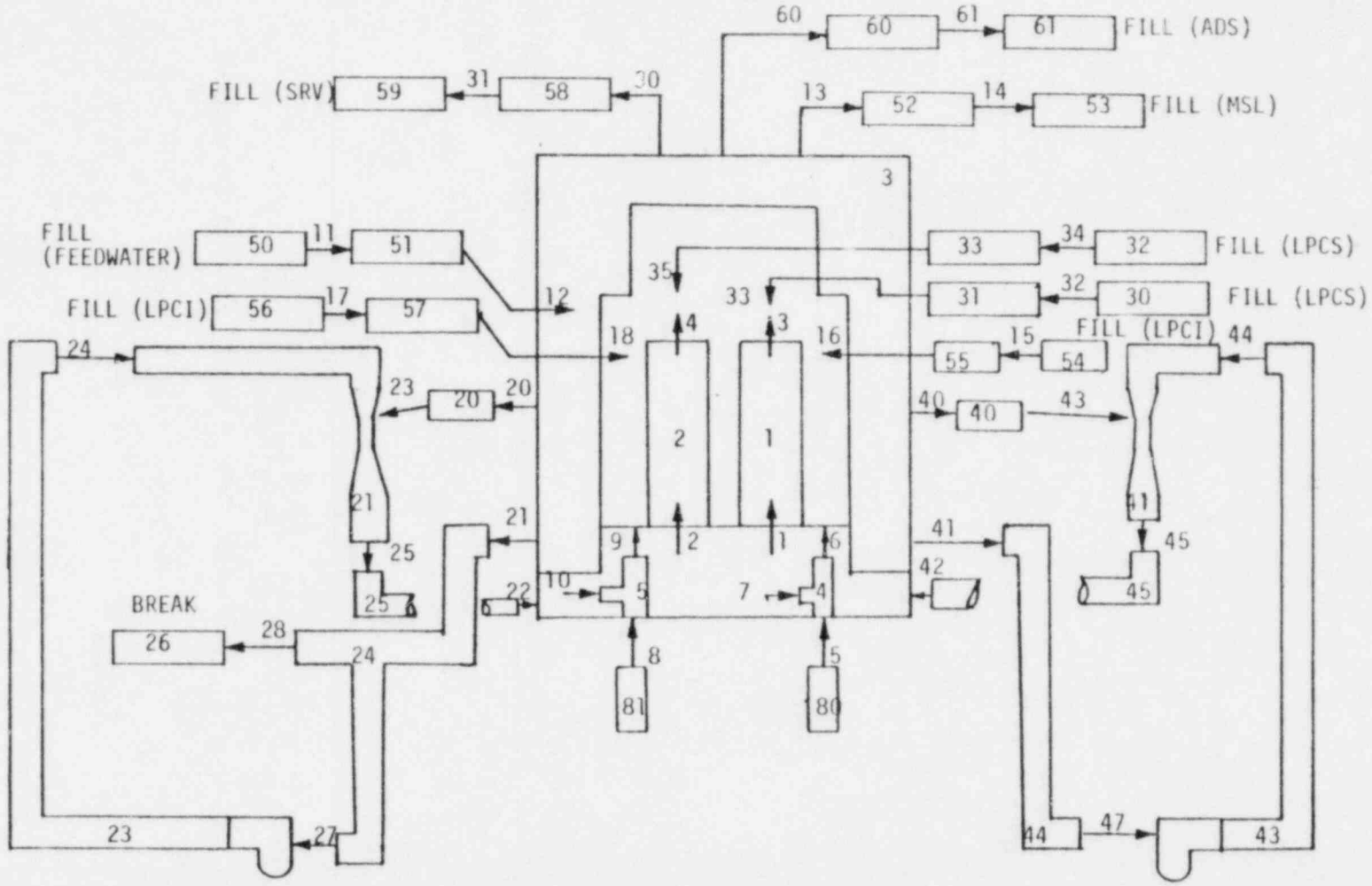

Figure 9. TRAC-BD1 system nodalization of ROSA-III.

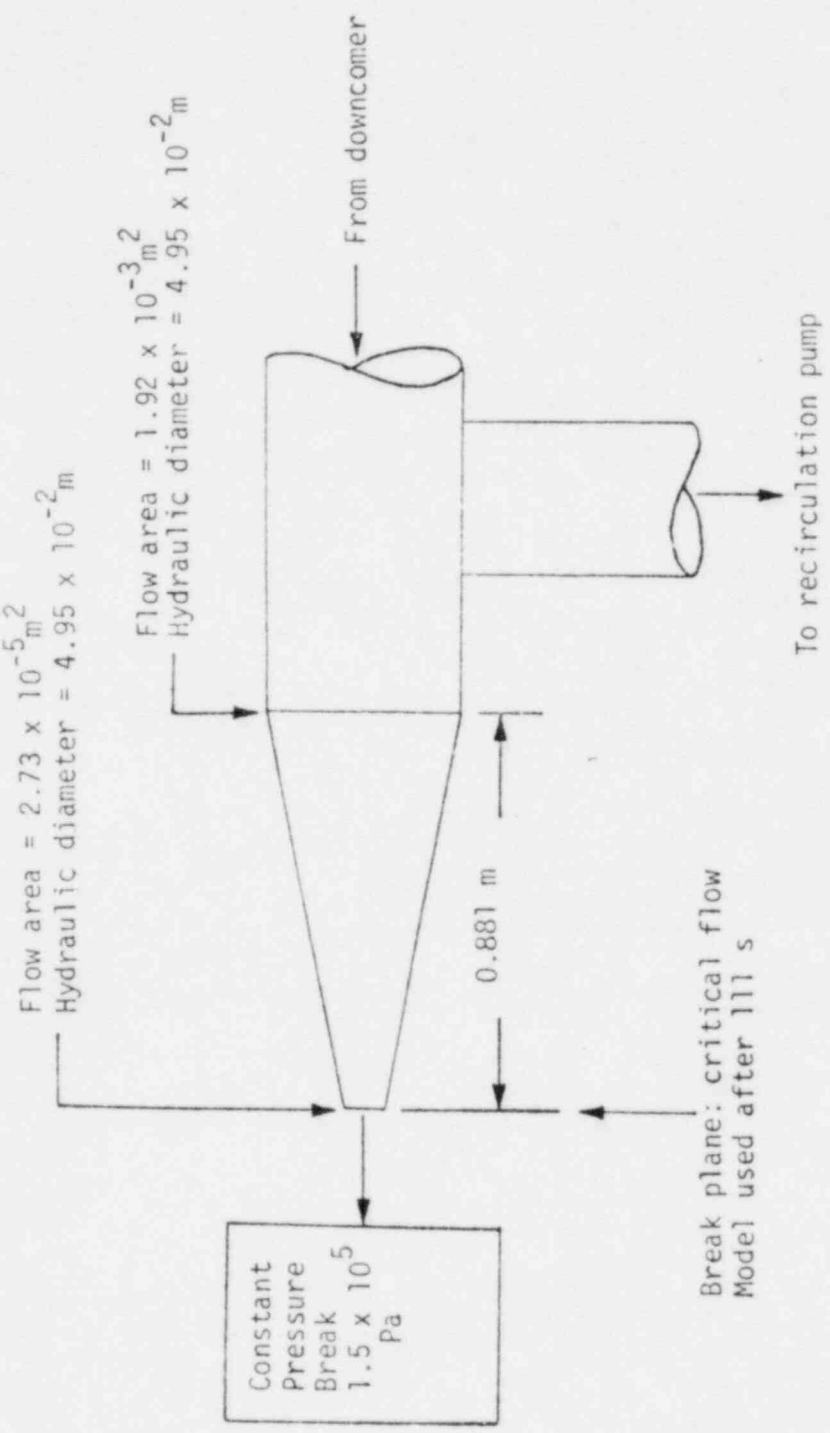

Figure 10. TRAC-BD1 break nodalization.

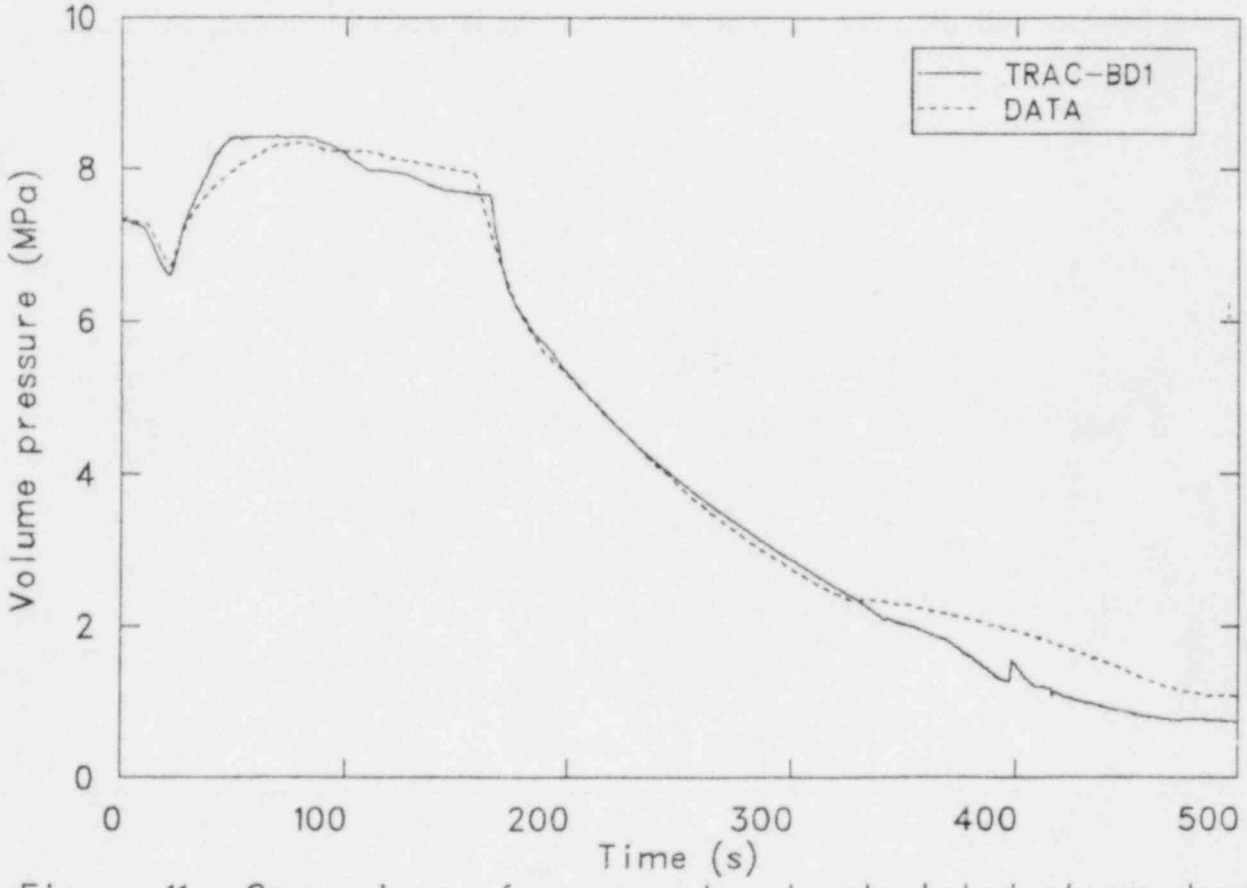

Figure 11. Comparison of measured and calculated steam dome pressure.

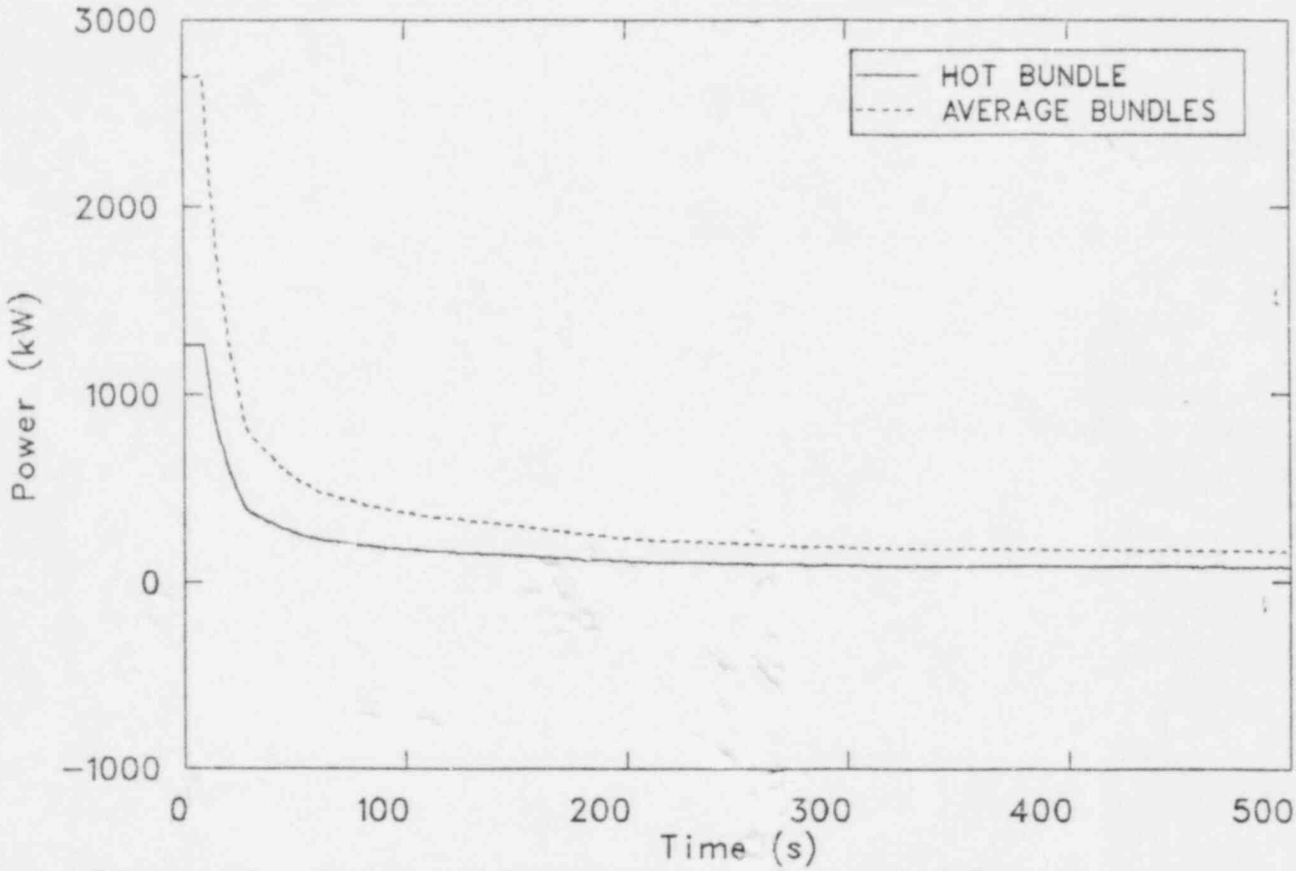

Figure 12. Measured bundle power for Run 912.

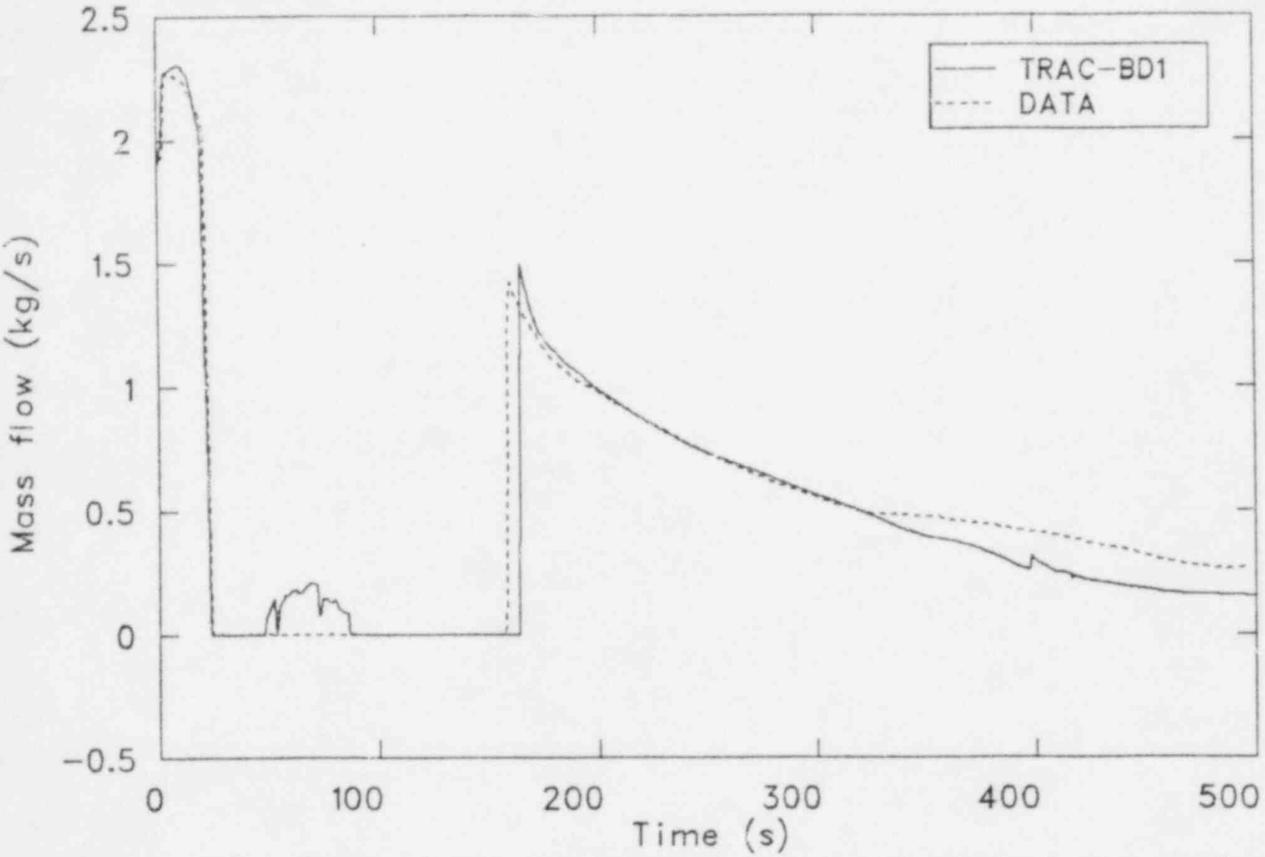

Figure 13. Comparison of measured and calculated steam line mass flows.

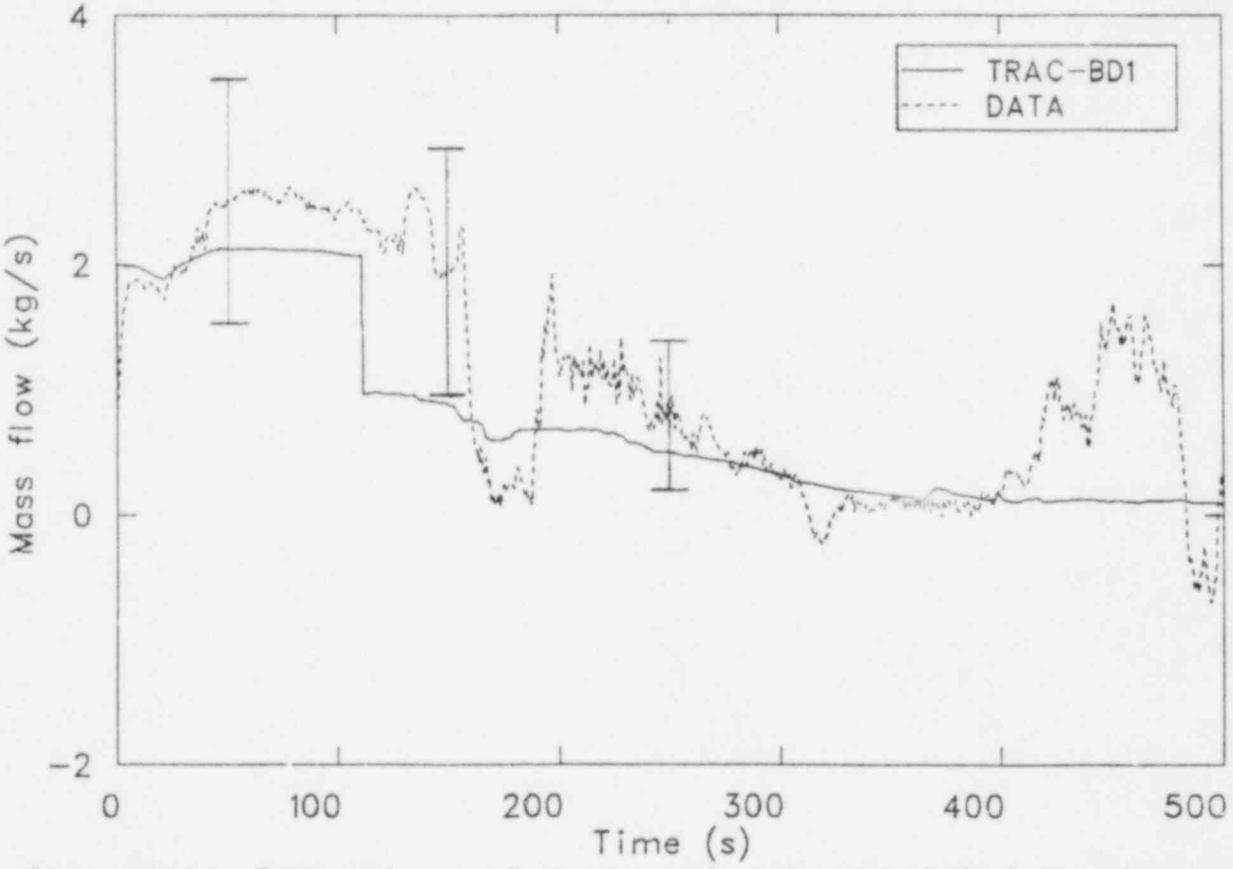

Figure 14. Comparison of measured and calculated break mass flow.

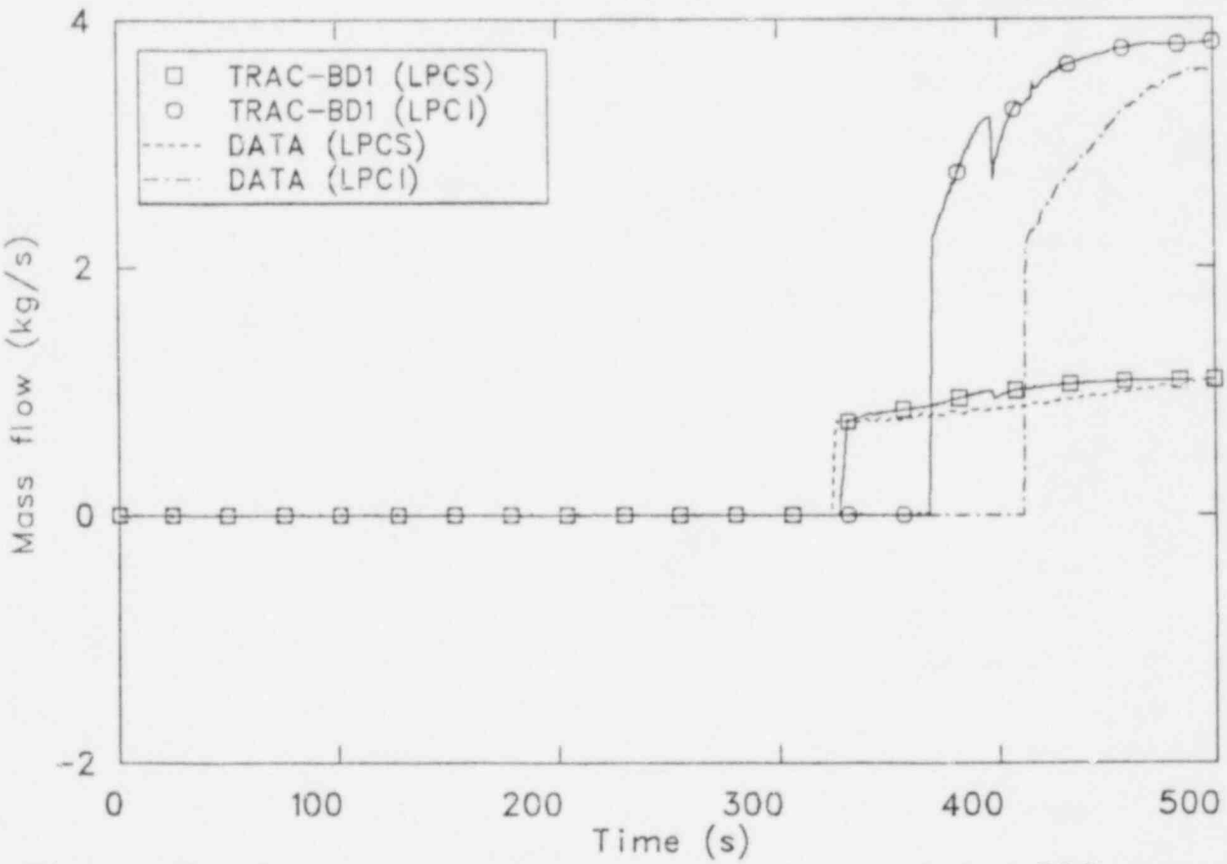

Figure 15. Comparison of measured and calculated ECC mass flows.

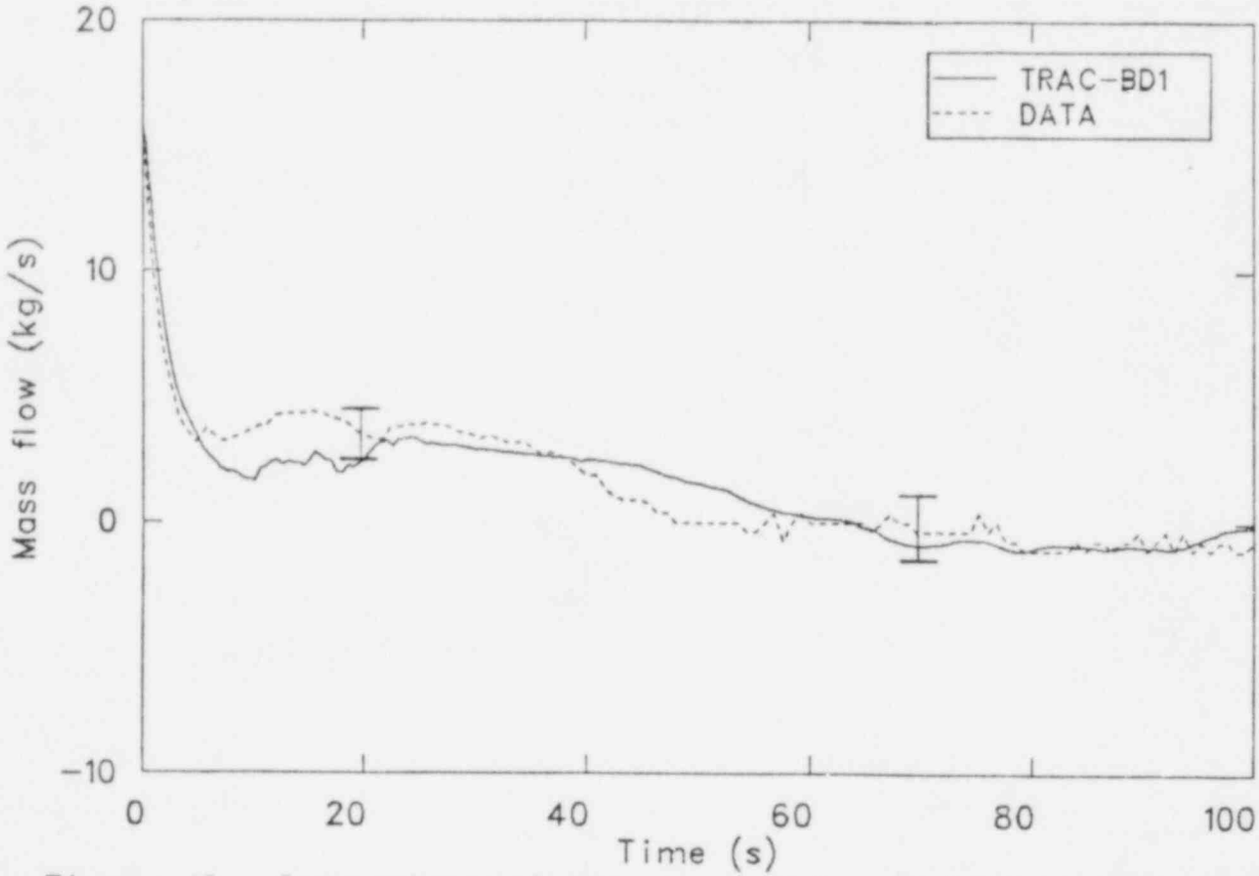

Figure 16. Comparison of measured and calculated core inlet mass flow.

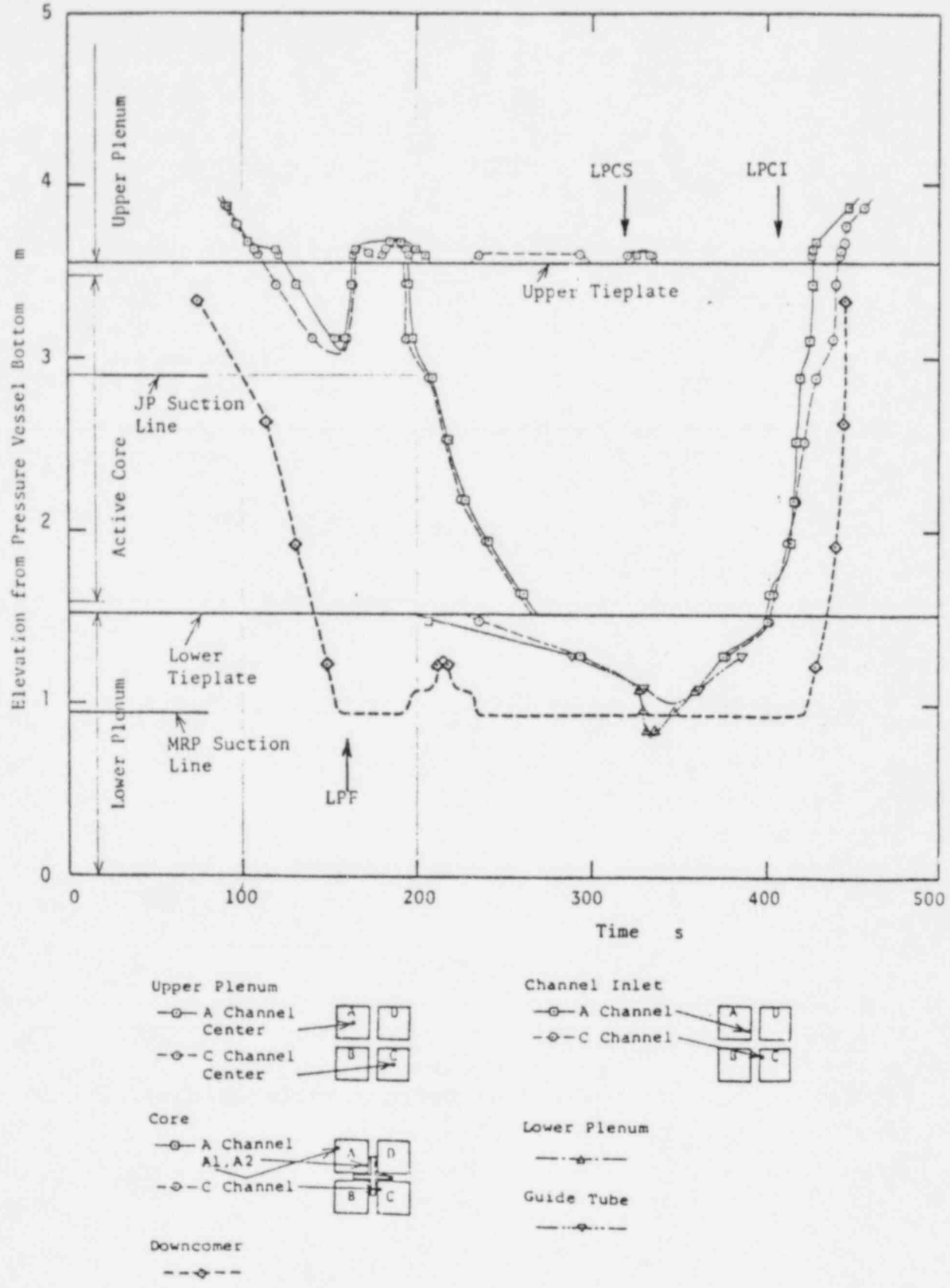

Figure 17. Estimated experimental liquid level in the pressure vessel.[3]

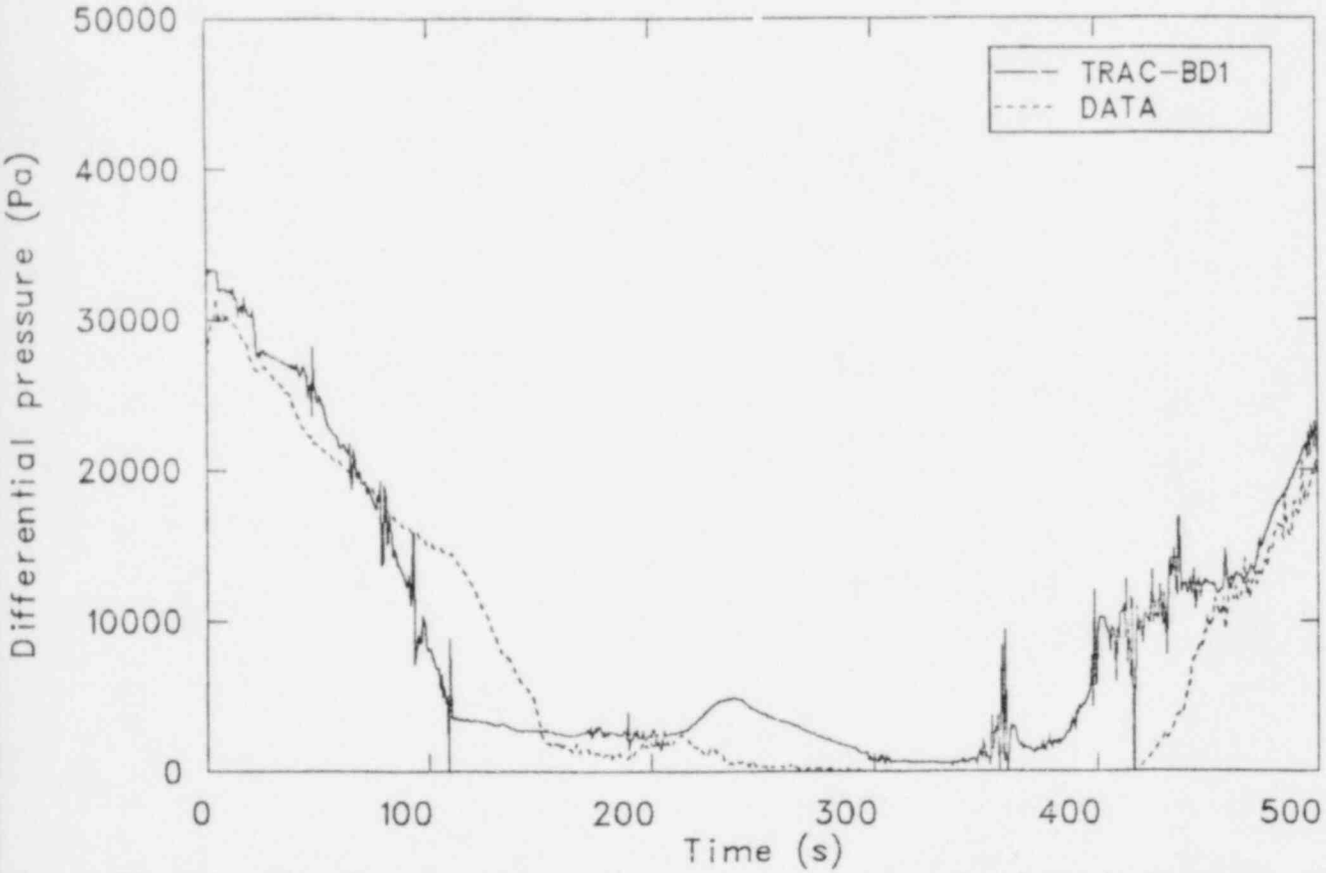

Figure 18. Comparison of measured and calculated downcomer head.

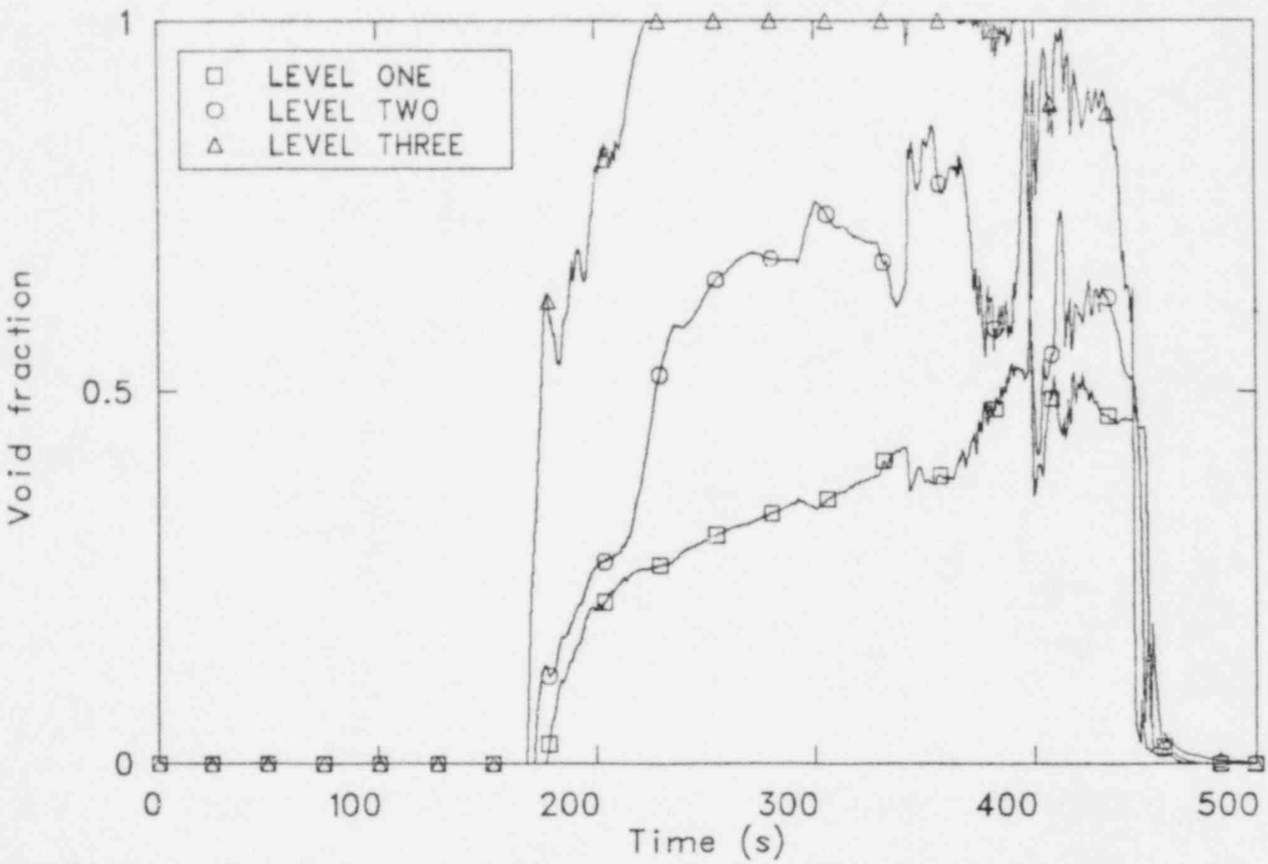

Figure 19. Calculated lower plenum void fractions.

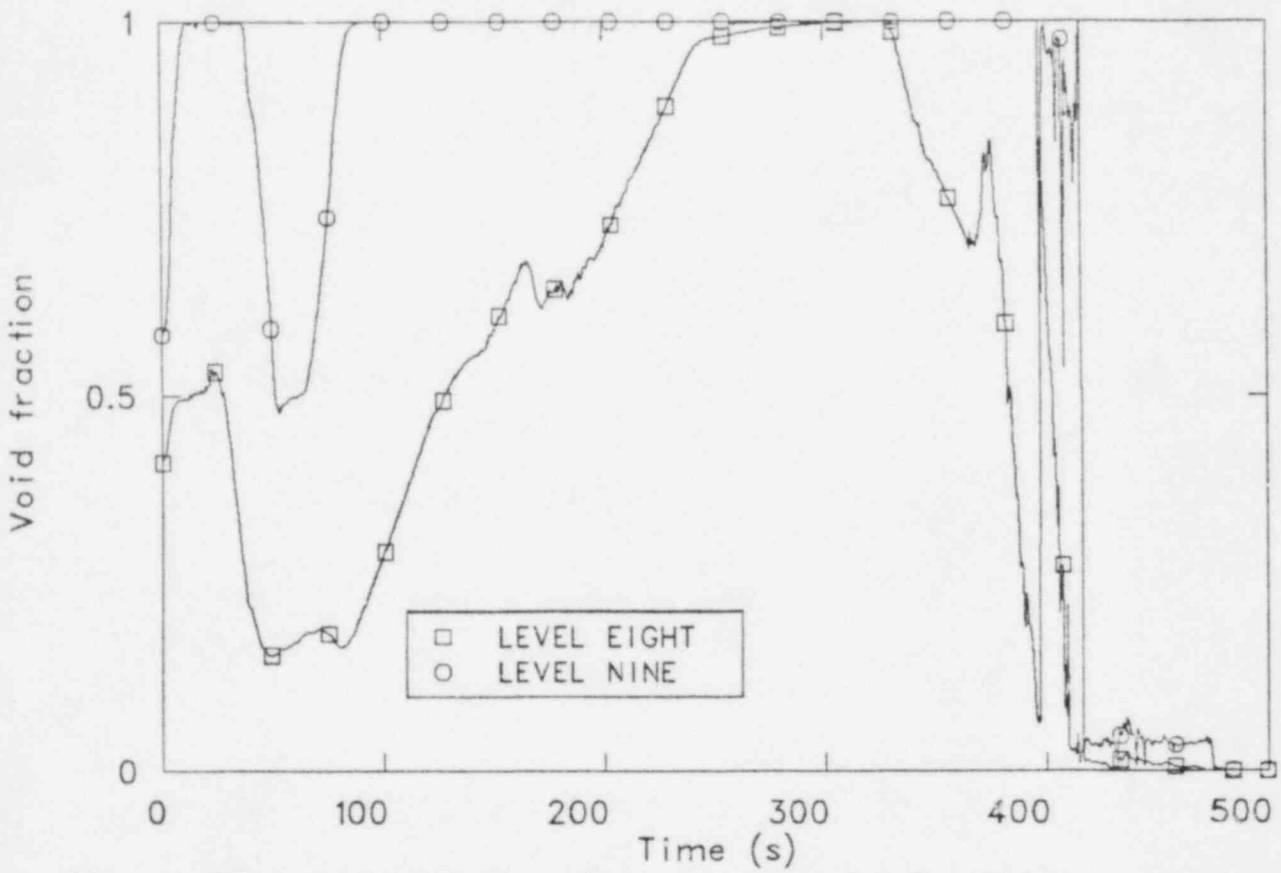

Figure 20. Calculated upper plenum void fractions.

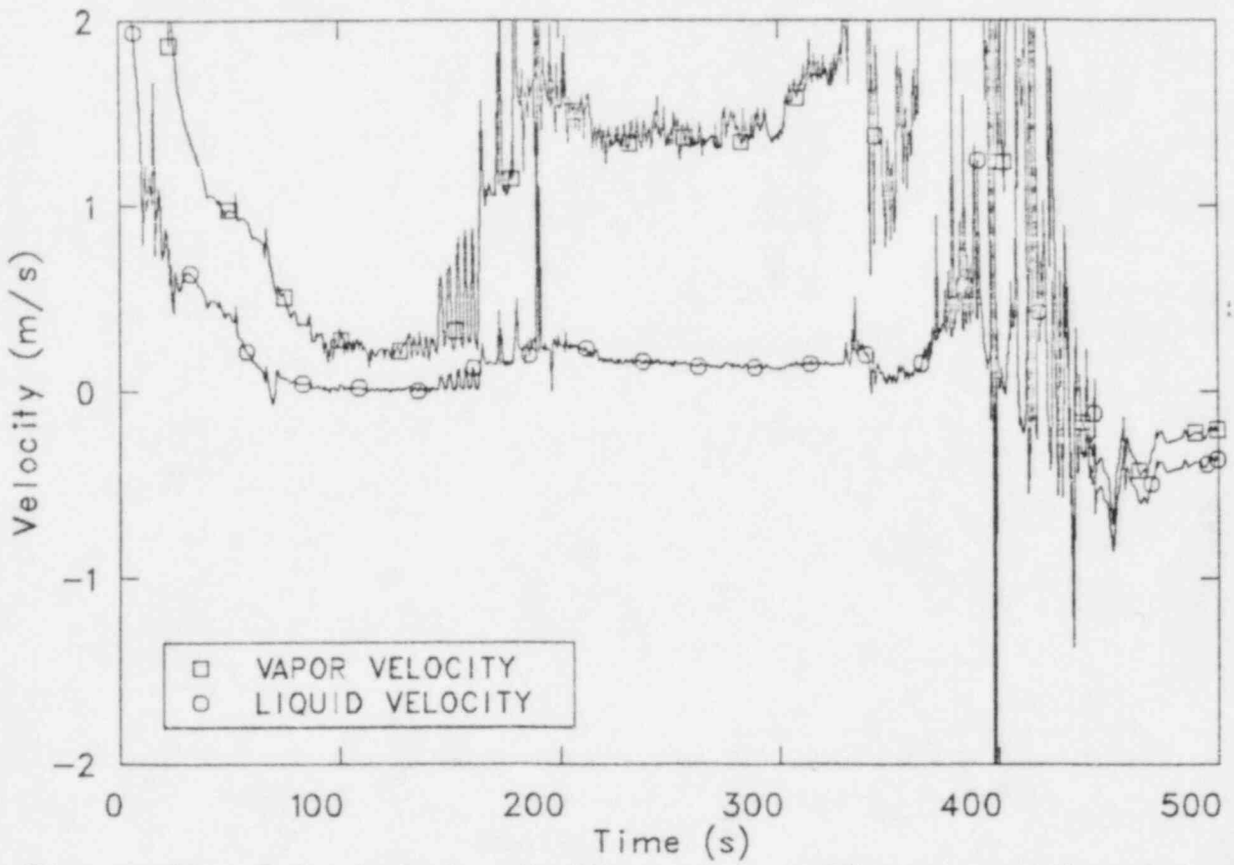

Figure 21. Calculated velocities at hot CHAN upper tie plate.

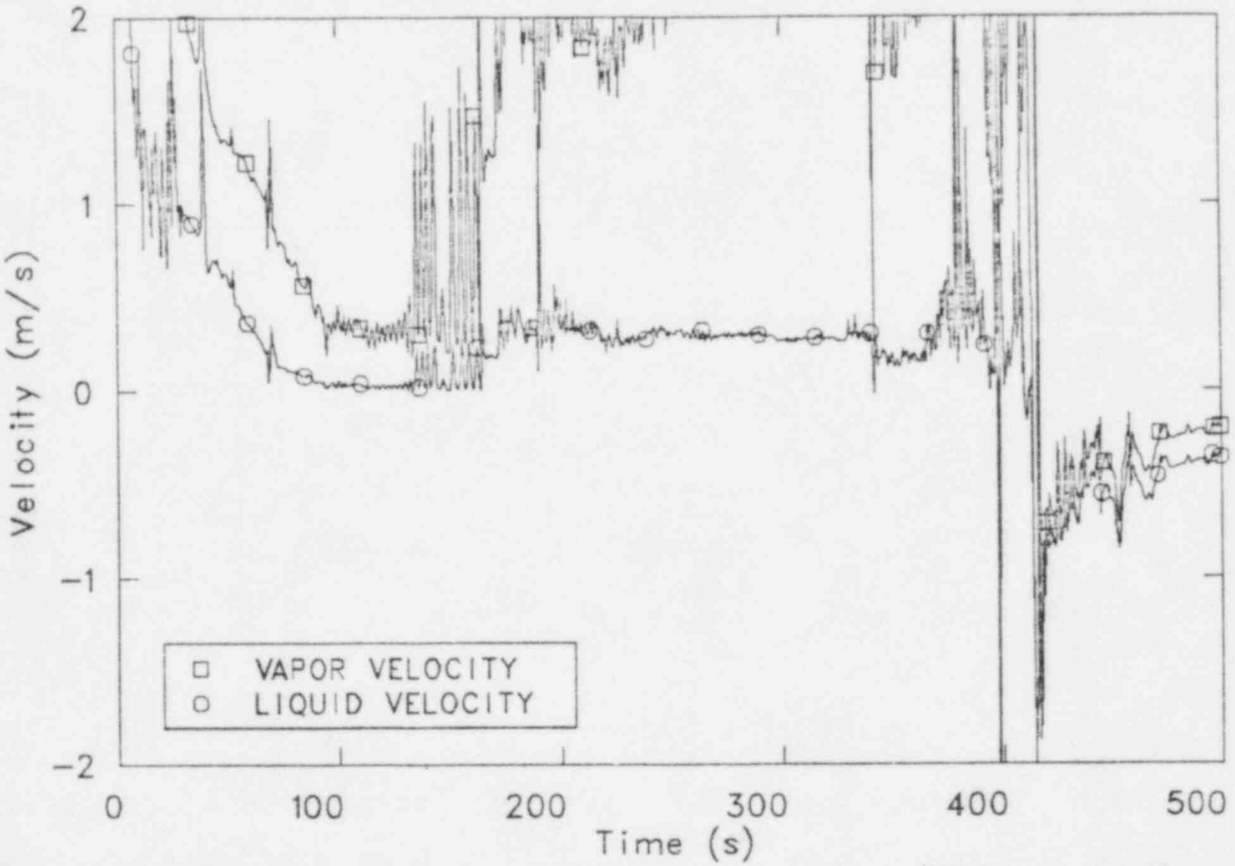

Figure 22. Calculated velocities at average CHAN upper tie plate.

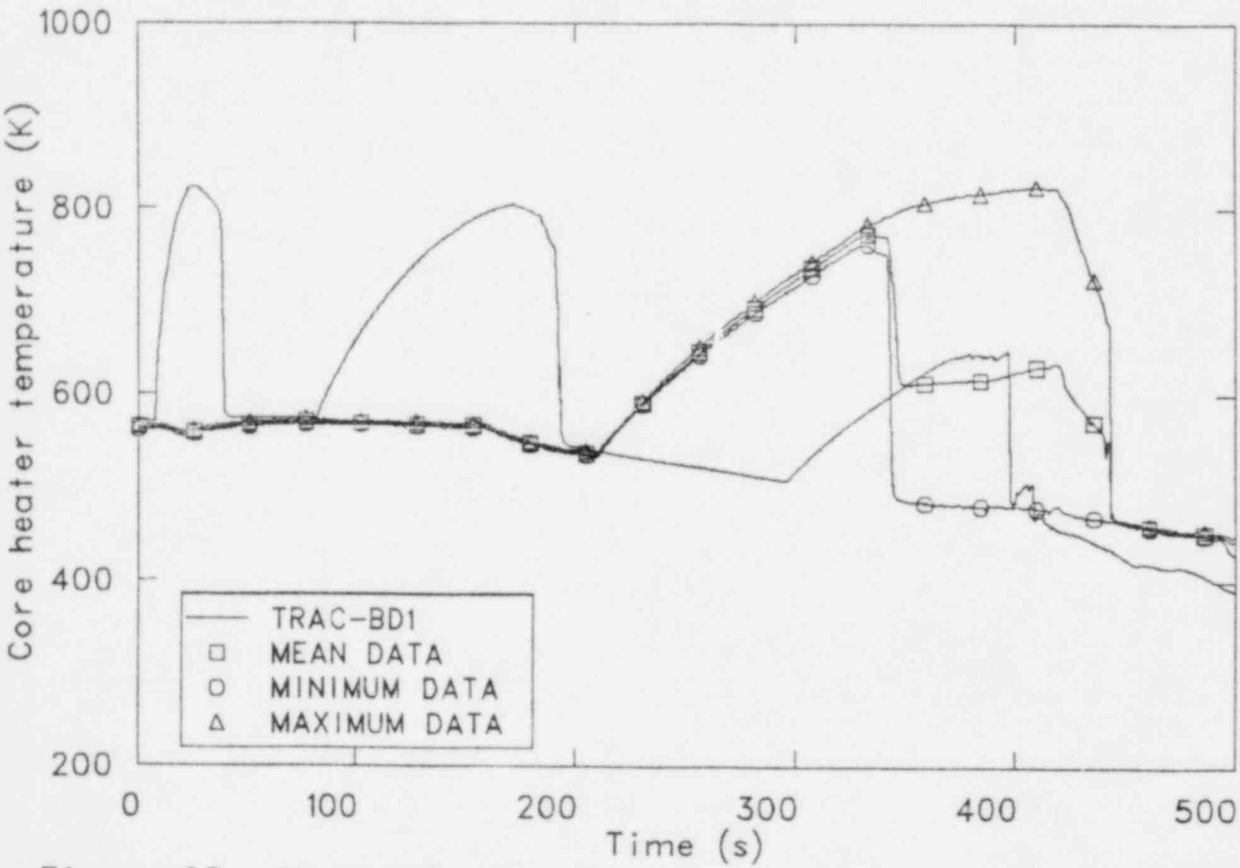

Figure 23. Measured and calculated rod temperatures in hot bundle position 3.

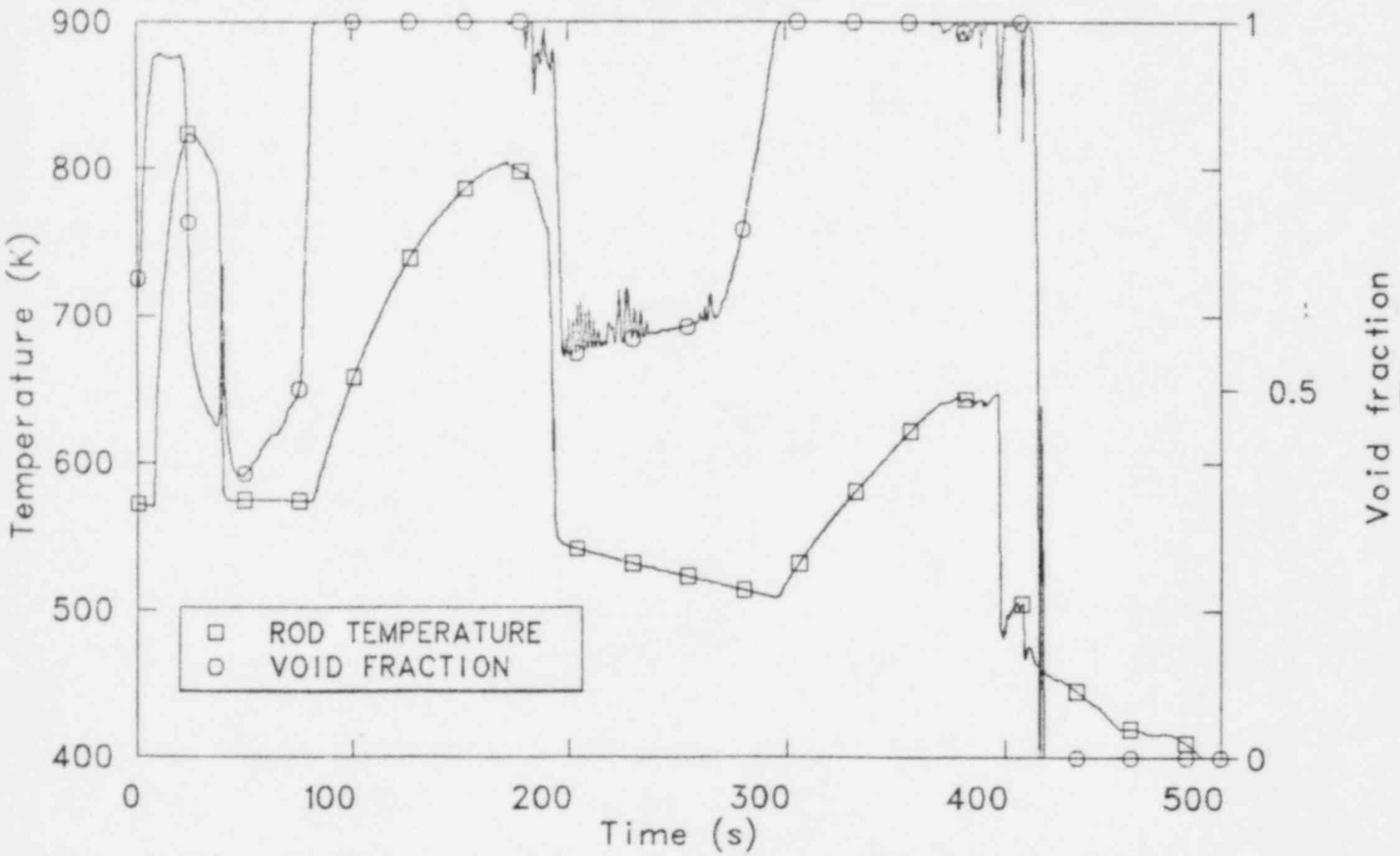

Figure 24. Calculated rod temperature and void fraction in hot CHAN position 3.

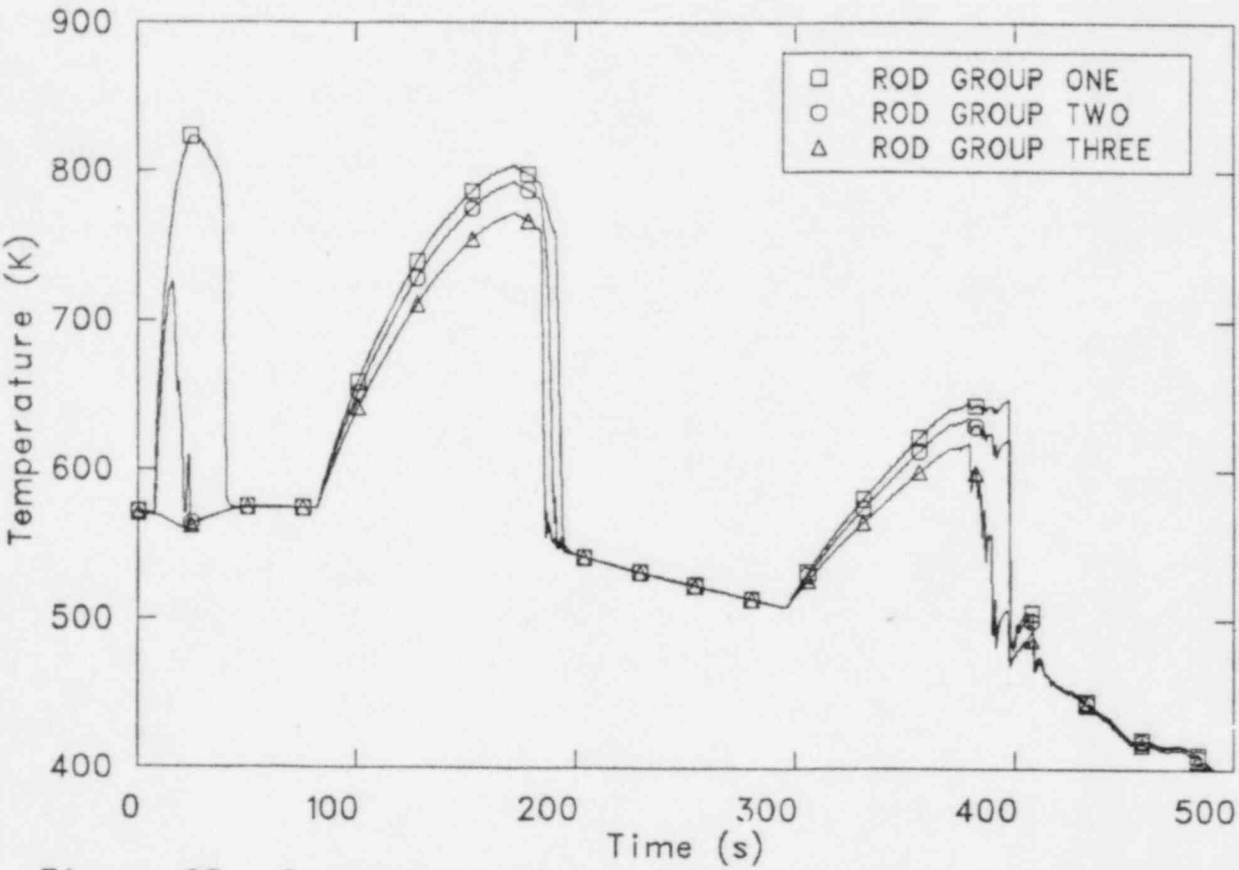

Figure 25. Comparison of hot CHAN rod group temperatures (position 3).

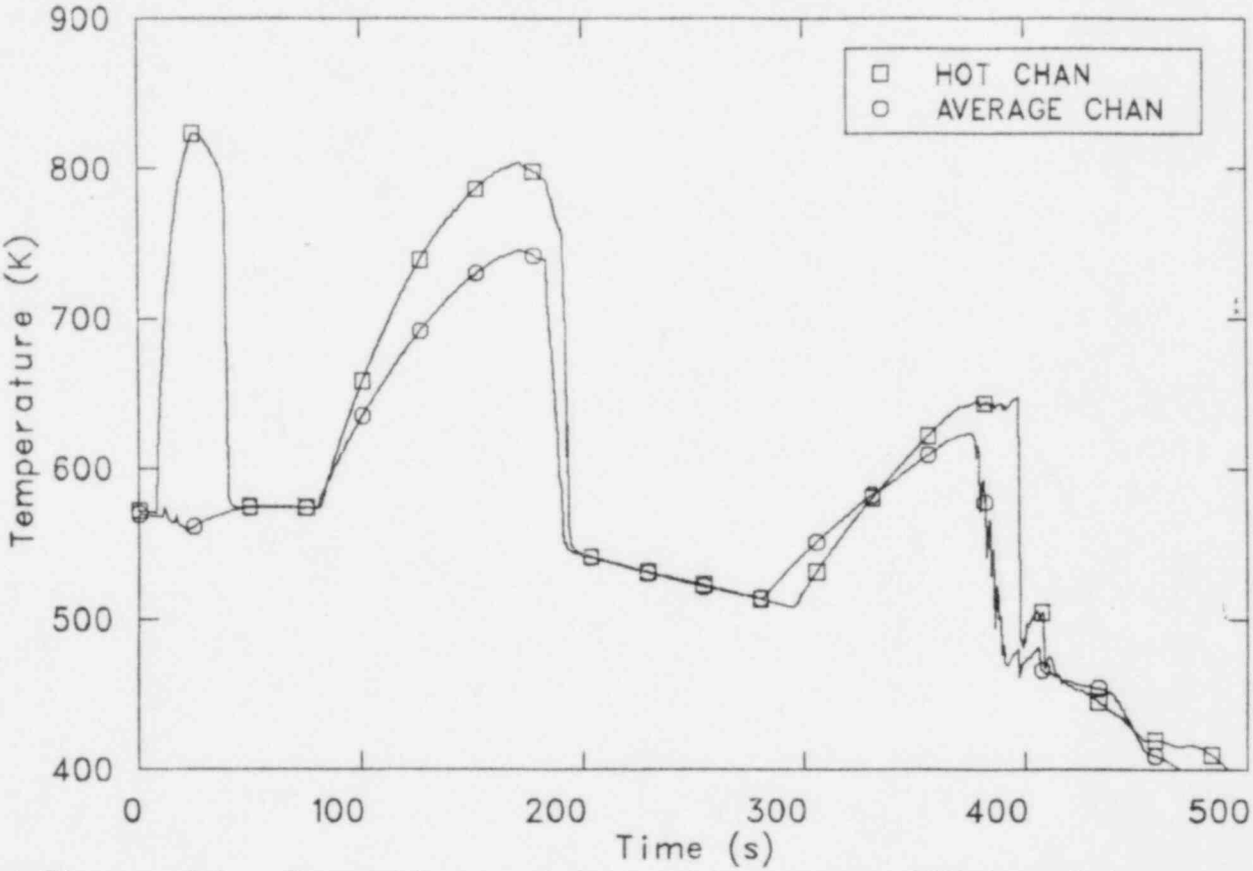

Figure 26. Comparison of hot and average CHAN rod temperatures (position 3).

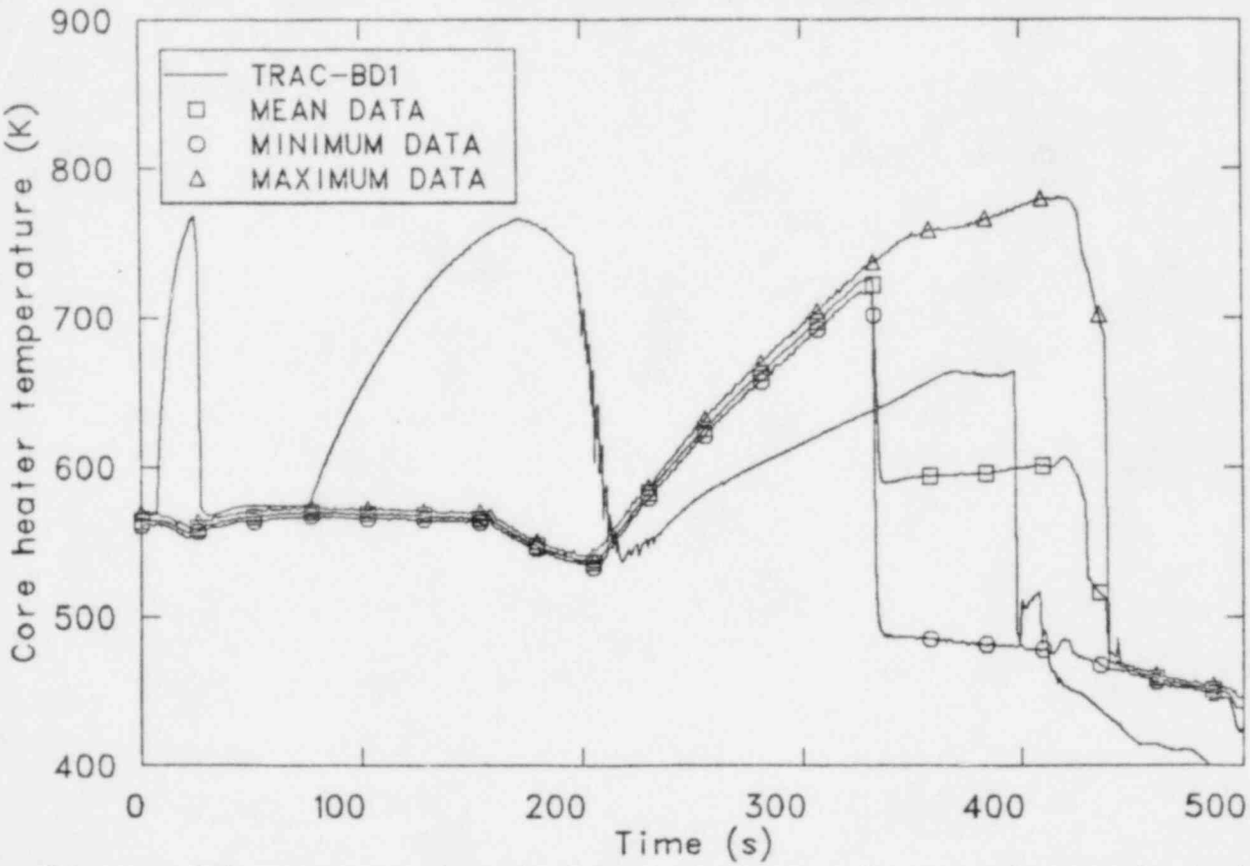

Figure 27. Measured and calculated rod temperatures in hot bundle position 2.

TABLE 1. INITIAL TEST CONDITIONS OF RUN 912

Parameter	Measured Value
Steam dome pressure (MPa)	7.30
Lower plenum temperature (K)	551.8
Lower plenum subcooling (K)	10.8
Core inlet flow rate (kg/s)	16.4
Core outlet quality (%)	13.5
Power level (kW)	1262 + 2707
Water level in vessel (m)	5.0
Feedwater temperature (K)	489
Steam line flow rate (kg/s)	2.04
ECCS coolant temperature (K)	313

TABLE 2. SEQUENCE OF EVENTS IN RUN 912[3]

Time after Break (s)	Events
0.0	Break Initiate core power control Terminate recirculation pump power
2.0	Initiation of feedwater line valve closure
3.1	Closure of feed water line
8.8	Initiation of core power curve reduction
19.0	L2 (4.76 m) signal
24.0	Closure of steam discharge line
38.2	L1 (4.25 m) signal
83.6	Safety relief valve actuation
98.8	Jet pump suction nozzle uncovery
117	Dryout at the top of the core
150	Recirculation pump suction nozzle uncovery
158	ADS valve opens (at system pressure 8.03 MPa)
159	Initiation of lower plenum flashing
275	Whole core uncovery
318	LPCS initiation (at system pressure 2.38 MPa)
406	LPCI initiation (at system pressure 1.81 MPa)
440	Completion of core reflooding
444	All heater rods quenched

APPENDIX A
TRAC-BD1 ASSESSMENT IMPLICATIONS

APPENDIX A
TRAC-BD1 ASSESSMENT IMPLICATIONS

The TRAC-BD1 calculation of ISP 12 provided code assessment information relative to TRAC-BD1's capabilities to predict an integral simulation of a small break LOCA. Key calculated qualitative parameters were compared to data in Section 4. Table A-1 contains comparisons of measured and calculated quantitative parameters.

An indication of how fast a computer code runs is found by taking the ratio of central processor (CP) seconds divided by transient seconds. For the present calculation, this ratio was 65:1. During mild parts of the transient the code ran faster (40:1), while during core reflood it was slower (91:1). The maximum time step size was user specified at 0.010 s. Figure A-1 shows the time step size used by TRAC-BD1 during the ISP 12 calculation. As would be expected, the code ran faster at larger time steps Courant limiting kept the time step size below the maximum during most of the transient. However, between 200 and 285 s the Courant-limited time step maximum was approximately 0.018 s. Therefore, for that time period, the code would have run faster had the maximum input time step been larger.

The code user can improve running time in two other ways. First, the larger the number of vessel cells contained in a model, the slower the code runs (the ROSA-III model contained 36 vessel cells). Decreasing vessel cells will improve running time. Second, by nodalizing the cells such that their length and volume are maximized, the Courant limit will be increased.

As stated in Section 3.1, the TRAC-BD1 version used for ISP 12 was very nearly the same as Version 12 of the code. However, two differences were present which could dramatically change results if ISP 12 were run with Version 12. First, an error was corrected in Version 12 that effected the calculated virtual mass term. The error correction resulted in higher values of calculated relative velocities. Second, in the intermediate version used for ISP 12 the interfacial drag coefficient was increased by a factor of $[1/(1-\alpha)]^{1/4}$. This forced the relative velocity to go to

zero as the void fraction went to one. This factor was taken out in Version 12, and this now serves to increase values of the relative velocity. It is suspected that these two changes would result in a better prediction of bundle fluid conditions, and consequently, heater rod temperatures.

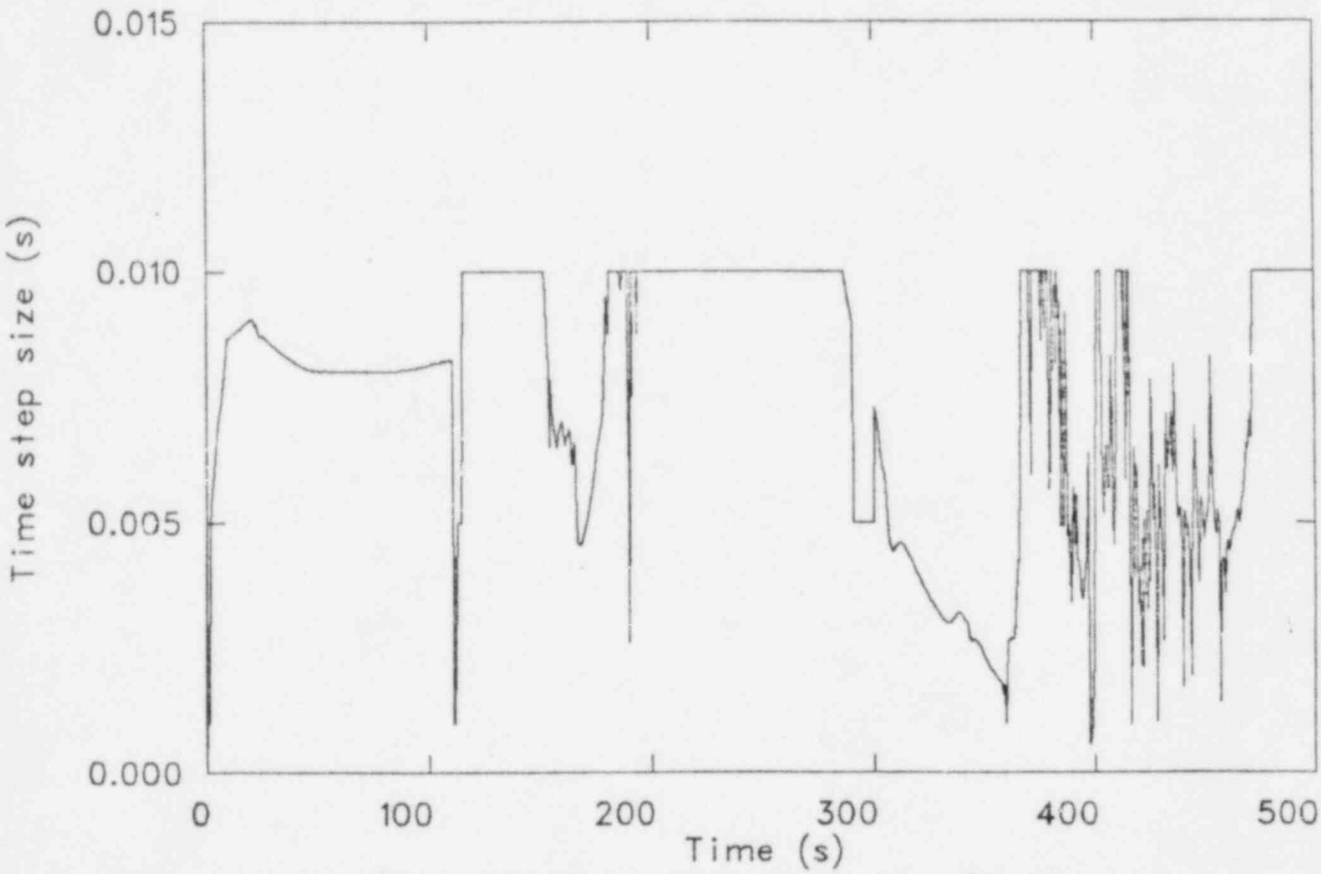

Figure A–1. TRAC–BD1 time step size for ISP 12.

TABLE A-1. COMPARISON OF MEASURED AND CALCULATED QUANTITATIVE ASSESSMENT PARAMETERS

Parameter	Data	TRAC-BD1
Peak clad temperature (K)	839	665[a]
Time to peak clad temperature (s)	410	397[a]
Time to initial rod dryout (s)	130	7
Time to core quench (s)	444	410
Time to jet pump suction uncovery (s)	100	80
Time to recirculation suction uncovery (s)	150	111
Time to ECCS initiation (s)		
ADS	158	164
LPCS	318	327
LPCI	406	367
Minimum downcomer differential pressure (Pa)	0-630[b]	500
Time to minimum downcomer differential pressure (s)	300	335

a. Early calculated temperature excursions were disregarded. As explained in Section 4, early calculated heatups did not occur in the data.

b. 630 Pa is the measurement uncertainty of the differential pressure transducer.